AD-A173 669 STRESS CORROSION OF CERAMIC MATERIALS(U) NATIONAL BUREAU OF STANDARDS GAITHERSBURG MD CERAMICS DIV S W FREIMAN ET AL 01 AUG 86 N00014-85-F-0021 1/1

UNCLASSIFIED F/G 11/2 NL

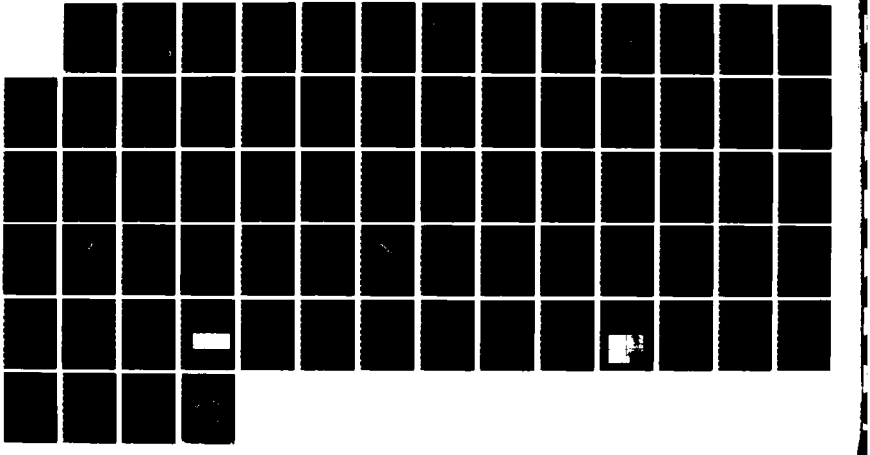

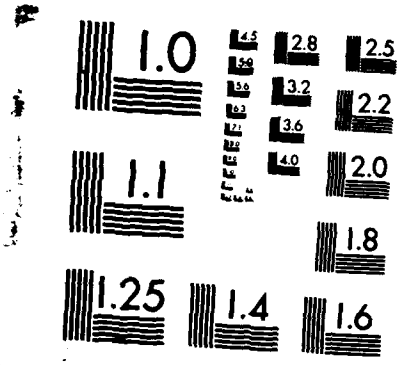

8

STRESS CORROSION OF CERAMIC MATERIALS

S.W. Freiman, G.S. White, T. L. Baker
S.M. Wiederhorn, T. D. Coyle, and L. Chuck

Annual Report

October 1, 1984 - September 30, 1985

ONR Contract No. N00014-85-F-0021

for

Office of Naval Research
Code 431
Arlington, VA 22217

by

National Bureau of Standards
Ceramics Division
Gaithersburg, MD 20899

August 1986

STRESS CORROSION OF CERAMIC MATERIALS

SUMMARY

The work during fiscal year 1985 can be divided into two distinct areas, namely (1) environmentally enhanced fracture of single crystals and glasses including effects of solution chemistry, and (2) fracture behavior of ceramics used in multilayer capacitors. The results of these investigations are summarized as follows:

(1) Environmentally Enhanced Crack Growth

A. Single Crystals

During this past year, fracture energy, γ, was determined on a series of single crystals of II-VI and III-V compounds as well as on a number of heavy metal fluoride glasses. The data was obtained through the use of an indentation-crack length procedure in which a Vickers indentation is placed in the surface of the material and the length of cracks emanating from the indentation are measured. This procedure can be performed either under inert environments (dry oil) or under more active liquids (water, formamide). Crack length was measured as a function of time after indentation.

No change in crack length with time was observed in the single crystal materials under an inert environment. The absolute values of γ measured for fracture on the cleavage plane in the particular material are in excellent agreement with those calculated using a fairly simplistic model derived by Gilman a number of years ago. In order to compare the effects of atomic bonding in the solid on fracture energy, the data were plotted as a function of the degree of ionicity in the bond. The fracture energy values were normalized by γ_o which is a function of the size of the atoms

which rupture at the crack tip in order to eliminate effects of atom size. As seen in Figure 1, fracture energy for this isostructural series of compounds decreases monotonically with ionicity. It appears in this plot that fracture energy should go to zero at an ionicity of about 0.8. This turns out to be the point at which the diamond cubic structure becomes unstable.

Initially, it was thought that environmentally enhanced crack growth could be characterized by the time dependence of the crack length after the indentation load was removed from the specimen. However, it was experimentally observed, and confirmed through calculations, that for N values greater than about 30, almost all crack extension would take place before the specimen could be placed in the microscope, i.e. 45 sec. Despite this problem, it was possible to compare the relative sensitivity of the different materials to the various environments by measuring the crack length after the same elapsed time in an environment relative to that in dry oil. This data is presented in Figure 2 as the ratio of the crack length in the particular environment after 15 minutes, C, normalized by that in dry oil for the same indentation load, C_0. The results indicate that both acetonitrile and water significantly enhance crack growth in partially or wholly ionic materials, i.e. GaAs, ZnS, and MgF_2. The lack of enhanced crack growth in heptane indicates that water dissolved in a relatively inert liquid will not produce longer cracks than occur in drier environments, and leads one to the conclusion that the acetonitrile and not the water dissolved in it is causing the enhanced crack extension. It appears that the more ionic solids such as MgF_2 are more sensitive to acetonitrile, in agreement with the findings of Michalske, Bunker and Freiman. Silicon shows anomalous behavior in that

no environment produces enhanced crack growth. This data suggest that water actually retards crack growth in silicon, but more work in this area is needed.

B. Fluoride Glasses

Similar environmentally enhanced crack growth studies were conducted on the heavy metal fluoride glasses whose compositions are given in Table 1. The overall behavior of these glasses is similar to that of the single crystals, namely environmentally enhanced crack extension occurs in water and acetonitrile. Unlike the single crystals, however, there is a small amount of crack growth in heptane compared to the oil. In addition, although the absolute crack lengths were much shorter in oil, some crack growth with time was observed. There appeared to be an order to the response of the various fluoride glass compositions. For instance, Glass 2 consistently exhibited more crack growth in each environment than did the others. Glass 6 seemed to undergo less environmentally enhanced crack growth. At present, however, we can not point to any one compositional variable which would account for this difference in behavior. Critical fracture toughness determined by the crack length technique described for the single crystals does not vary appreciable from one composition to another (Table 1).

C. Solution Chemistry

In addition, during this past year a study was undertaken to determine the effects of counter-ions in aqueous solutions, e.g. Cs^+, K^+, Na^+, and Li^+, on crack growth behavior in vitreous silica. At a pH < about 12, no effects of varying concentrations of these ions could be measured. At higher pH, it was observed that in solutions containing 1 mole/liter of Li, crack growth rates were about an order of magnitude lower for the same

K_I. No effects of the other ions were observed. The effect of Li in lowering crack growth rates in silica was ascribed to its propensity to combine with OH ions, thereby preventing them from participating in the crack tip reaction. Lithium tends to be much more associated with OH in high concentrations than the other ions in this series. Based upon these results it was predicated that other elements which tended to associate with hydroxyl ions would behave in a similar manner. Experiments conducted in thallium (Tℓ) solutions confirmed this prediction.

(2) Fracture of Capacitor Ceramics

Indentation-fracture techniques were used to determine the effects of composition and microstructure on strength and environmentally enhanced crack growth in a number of ceramic materials used in multilayer capacitors. The critical fracture toughness of these materials was shown to be quite variable from one type of capacitor designation to another. Differences are ascribed to variations in both microstructure and grain boundary chemistry. The effects of internal stresses observed in transducer ceramics are much smaller in these materials, probably because of the more diffuse nature of the paraelectric to ferroelectric phase transformation. Nevertheless, strength levels measured at small indentation loads could be correlated with dielectric aging rates in two different capacitor ceramics, i.e., the greater the internal stress, the higher the aging rate. The magnitude of these internal stresses did not appear to change with time.

Susceptibility to moisture enhanced crack growth, as determined from the slopes of dynamic fatigue curves, was also shown to be a strong function of capacitor composition. The shape of these dynamic fatigue plots for two X7R compositions suggested the existence of a crack growth

limit in these materials. This type of crack growth data has been shown to be useful in the prediction of safe operating conditions for these materials.

TABLE 1

Composition and Properties of Fluoride Glasses

COMP #	ZrF_4	HfF_4	BaF_2	LaF_3	AlF_3	$(RE)F_3$	ThF_4	Other	K_{Ic}
2	60.5	-	33.5	3.5	2.5	-	-		.36
3	57	-	35	5	3	-	-		.34
4	55.5	-	33	5	5.5	4.1	-		.37
5	58.1	-	34.2	-	3.6	-	-	Gd	.33
6	59	-	32.8	-	3.6	-	4.6		.34
7	58	-	34.5	-	4.5	3	-	H_o	.32

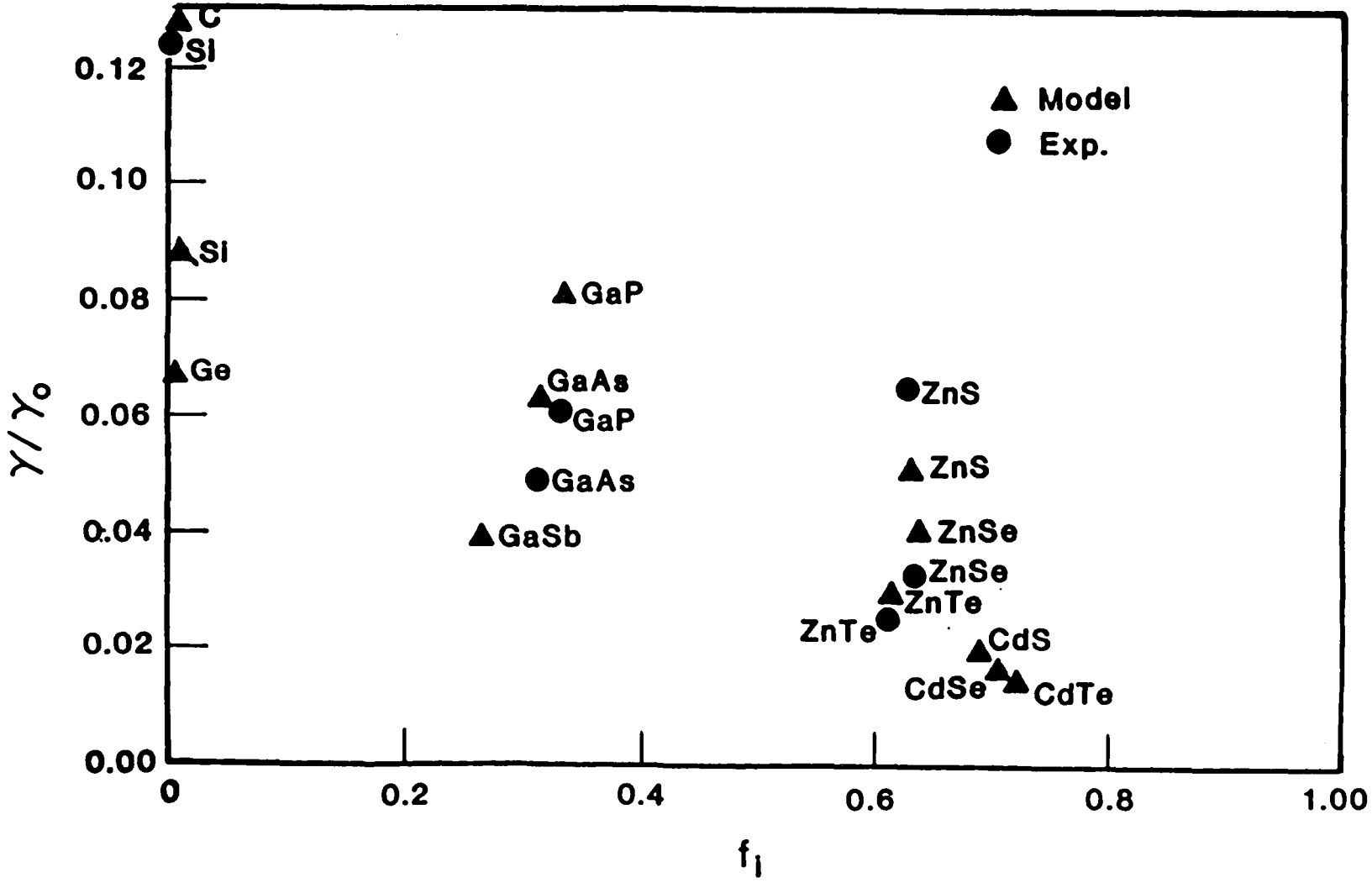

Figure 1. Experimental and calculated fracture energies for single crystals as a function of ionicity, f_i. All γ values have been normalized by a parameter, γ_o, which accounts for the ionic size variation from one compound to another.

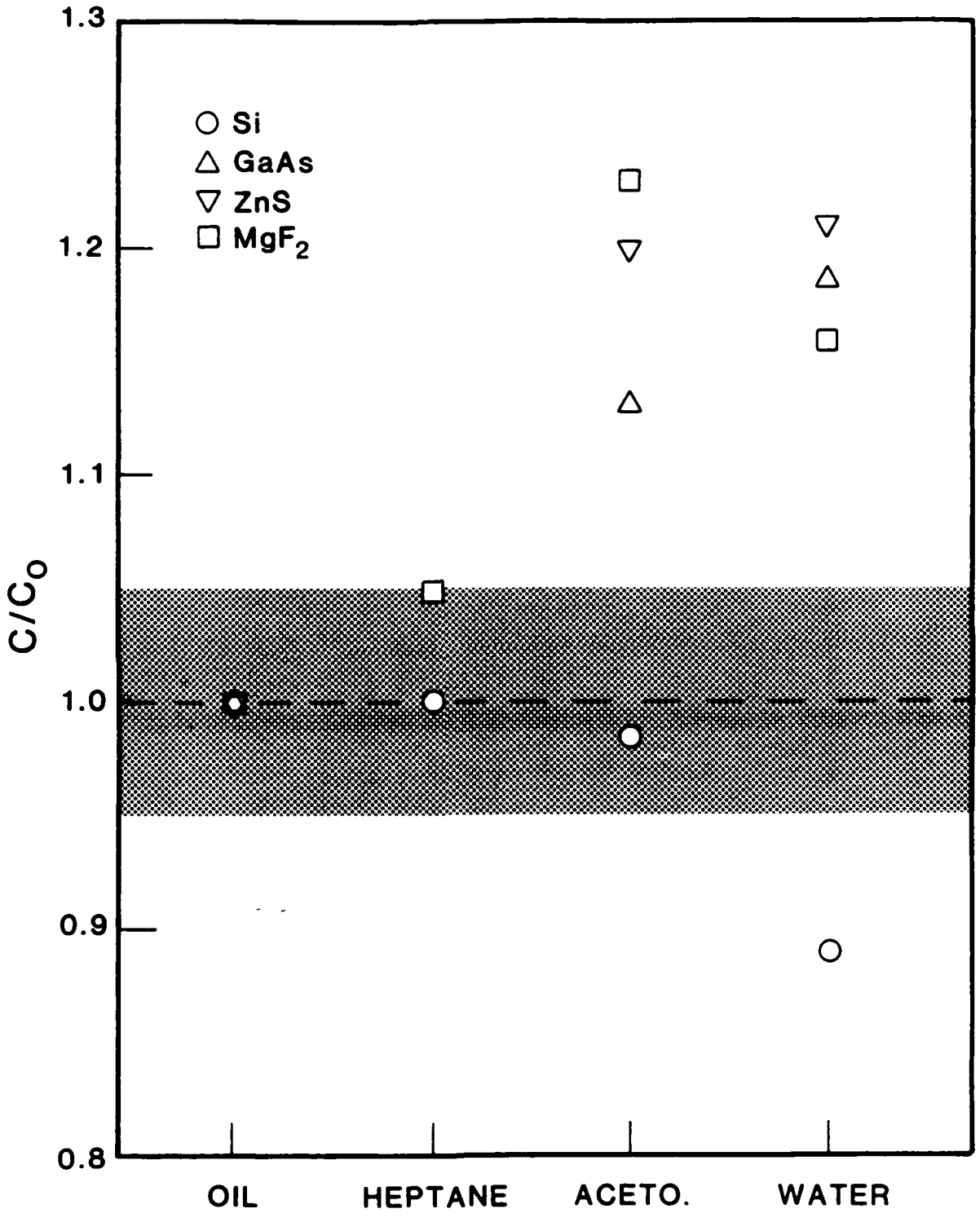

Figure 2. Crack length, C, for compounds in various environments. C_o is crack length in dry oil. Crosshatched region represents the error band.

EFFECTS OF COUNTER IONS ON CRACK GROWTH IN VITREOUS SILICA

G.S. White, S.W. Freiman, S.M. Wiederhorn, and T.D. Coyle
National Bureau of Standards
Gaithersberg, Md. 20899

ABSTRACT

Crack growth studies on silica glass were conducted as a function of pH in the range 1 to 14. The slope of the crack growth data were found to be steeper in acidic and neutral solutions than in basic solutions. Of four alkali metal hydroxide solutions studied, only lithium hydroxide behaved differently from the others and only in concentrated, ≥1 M, solutions. At this concentration, the slope and position of the crack growth curve for LiOH were typical of that obtained in acidic or neutral solutions. From an analysis of the data in terms of a surface force model of crack growth, we suggest that surface forces have a similar range and magnitude to the cohesive forces that bind the silica together. As a consequence of these large forces, we also suggest that the influence of alkali metal hydroxides on crack growth is largely chemical in nature, involving short range forces associated with the breaking of bonds at the crack tip. Two mechanisms for chemical attack are considered: in basic solutions the siloxane bonds at the crack tip are believed to be attacked directly by the hydroxide ions in solution; in acidic or neutral solutions the siloxane bonds are believed to be attacked by water in the electrolyte. Lithium hydroxide behaves differently from the others because lithium ions associate with hydroxide ions, reducing the effective activity of the hydroxide ions at the crack tip.

1. Introduction

By now there is general agreement that crack growth in silicate glasses is normally caused by water in the environment[1]. Water at crack tips reacts chemically with strained siloxane bonds resulting in bond cleavage and, as a consequence, crack advance. In gaseous, or nonaqueous environments, the reaction rate appears to be solely determined by the chemical activity of the water in the environment [2, 3]. By increasing the chemical activity of the water, crack motion for a given applied stress intensity factor, K_{Ia}, is also increased. Thus, it makes little difference if crack growth measurements are made in air, or in nonpolar solvents; the position and slope of the crack velocity curve is determined solely by the relative humidity (i.e. the relative chemical activity) of the test environment [3].

In aqueous environments, the situation is somewhat different, since crack growth is also sensitive to the hydrogen ion activity, i.e. the pH, of the environment [4]. If the logarithm of the crack velocity is plotted as a function of the applied stress intensity factor, the slope of the crack velocity curve is greater in acidic environments than in basic environments. This conclusion holds for soda-lime-silica glass, chemical-borosilicate glass, and silica glass, suggesting the general validity of the result for silica based glasses. However, despite the fact that this result has been well documented, the reason for the sensitivity of crack growth to pH has never been explained at a fundamental level.

In this paper the relation between electrolyte composition and the position and slope of the crack velocity curve is further explored for vitreous silica. Since environmental pH is known to determine the magnitude of the electric charge on vitreous silica surfaces [5], the connection between crack growth behavior and pH might result from the charge that develops on the silica surface as a consequence of environmental pH. Surface charge can affect crack growth either by altering the chemistry of the bond-breaking reaction, or by determining the level of forces between the fracture surfaces as the crack propagates. If surface charges are important to crack growth, then both the concentration and type of counter ions on the fracture surfaces of the glass are expected to influence crack growth. With this in mind, a study was conducted to determine the affect of cation type and cation concentration on crack growth in vitreous silica.

2. Experimental Procedure

Crack growth studies on vitreous silica were conducted primarily on constant-moment, double-cantilever-beam specimens 12.5 mm wide, 50 mm long and 2 mm thick. To constrain the crack to the mid plane of the specimen, a groove 1.5 mm deep and 1 mm wide was ground into one surface of the specimen along the specimen mid plane. After grooving, specimens were annealed at 1200°C to remove residual stresses introduced by grinding. The specimens were then mechanically pre-cracked and subjected to a

constant (dead-weight) load to induce crack growth. Crack velocities were determined with an optical microscope using a filar eyepiece to plot the position of the crack as a function of time.

At least 10 data points were obtained in each environment to accurately represent the crack velocity curve. Specimens were usually long enough to obtain crack growth curves in several different environments. A procedure of comparing the position of $v\text{-}K_{Ia}$ curves obtained on a single specimen in several different environments was adopted since past experience [6] has shown this to be the most sensitive technique to evaluate small effects of environment on crack growth. The technique eliminated specimen-to-specimen scatter resulting from small variations in specimen geometry and specimen loading. To assure ourselves that the data from each environment were truly characteristic of the environment and not some artifact of the testing procedure, the order of testing in replicate studies was often changed, and sometimes two or more velocity curves on a specimen were obtained in an environment, with curves from one or more other environments in between.

Crack growth studies were conducted primarily in basic environments, pH $\geq$ 11, however some measurements were also made in distilled water and in acidic solutions, to compare the present set of data with an earlier set of data [4]. Initial studies were conducted in 0.001 M solutions of Li and K hydroxide and in 1 M solutions of Cs, K, Na and Li hydroxide. As these

studies proceeded, it became apparent that crack growth data obtained in solutions containing Li^+ ions differed from those obtained in solutions containing the other alkali metal ions. Therefore, additional crack growth curves were obtained in LiOH solutions and solutions containing mixtures of LiOH and other alkali metal hydroxides. Crack velocities were also measured in 1 M solutions of thallium(I) hydroxide, which behaves similarly to lithium hydroxide vis-a-vis ion association. The lithium ion concentration of the test solution was also used as a test variable in this study because ion concentration affects both the degree of charge formation at the silica surface [5] and the structure of the double layer [7] at the surface. Finally, the pH of all test solutions was measured using narrow range indicator paper and a pH meter.

3. Results

Typical crack growth data obtained in acidic, basic and neutral solutions are shown in figure 1, where the logarithm of the crack velocity is plotted as a function of the applied stress intensity factor. The crack growth data for each of the solutions can be represented by a straight line over the entire range of measurements. As noted earlier by Wiederhorn and Johnson [4], the slope of the curves is steeper in acidic than in basic solutions. Furthermore, the slope of the crack growth curve obtained in water is closer to that obtained in acidic than in basic solutions. In dilute basic solutions, 0.001 M potassium or lithium hydroxide, figure 2, the slope of the v-K_I curve is

approximately one-half that obtained in acidic solutions, suggesting an important role for the hydroxide ion in the crack propagation mechanism even at relatively low concentrations. Furthermore, since lithium and potassium hydroxide data fit the same curve at 0.001 M, cation type has little effect on crack growth behavior at such low concentrations.

In contrast to the above results in dilute hydroxide solutions, the type of cation seems to have an effect on crack growth in more concentrated hydroxide solutions, as is indicated in figure 3a, which compares the data from multiple runs in 1 M LiOH and 1 M KOH. For most of the range of data, the curve for the LiOH lies at a lower crack velocity and has a higher slope than the one for KOH. The separation of the two sets of data is beyond the range of scatter of the data used to determine each of the curves. At high velocities, 10^{-3} m/s, the two sets of data seem to merge, suggesting a change in crack growth mechanism. As can be seen from figure 3b, the curve for the crack velocity in 1 M LiOH is indistinguishable from the one for distilled water. The similarity between the v-K_{Ia} data taken in water and that taken in 1 M LiOH suggests that the kinetics and perhaps the mechanism for fracture in these two environments is the same. In contrast to these results, a comparison of the data obtained in 1 M CsOH, and 1 M NaOH with that obtained in 1 M KOH, figure 4, indicates little if any effect of cation type on the crack growth behavior. Therefore, of the four cations studied, only Li^+ behaves differently from the others.

To further quantify the effect of lithium ion on crack growth in vitreous silica, several auxiliary experiments were conducted. To test the effect of LiOH concentration, data were obtained in LiOH solutions that ranged from 0.001 M to 1.0 M. As shown in figure 5, crack growth data obtained in concentrations of 0.01 M and 0.1 M LiOH are indistinguishable from those obtained in 0.001 M LiOH solution. Between concentrations of 0.1 M and 1.0 M, the effect of Li^+ on crack growth is readily apparent, since the crack velocity decreases by almost an order of magnitude between these two concentrations.

To separate the role of lithium ion concentration from that of hydroxide ion concentration, a second set of experiments was conducted in 0.001 M LiOH solution to which sufficient $LiNO_3$ was added to bring the total concentration of Li^+ to 1 M. This study, figure 6, indicates no significant difference between the results obtained in 0.001 M LiOH and those obtained in the mixed solution. These results suggest that a high concentration of Li^+ by itself is not sufficient to modify the mode of crack growth from that usually obtained in basic aqueous solutions. A similar null result was obtained for a solution of 1 M KOH to which enough $LiNO_3$ was added to bring the total Li^+ to 0.001 M. Apparently, both the hydroxide ion concentration and the lithium ion concentration of the test environment must be substantial for Li^+ to influence crack growth.

Finally, the simultaneous effect of a second cation on the crack growth rate was tested by adding equal quantities of 1 M

KOH and 1 M $LiNO_3$. As can be seen from figure 7, the mixed cation solution behaved similarly to that of a 1 M LiOH solution suggesting that when the hydroxide ion concentration of the test environment is high enough, the full effect of the Li^+ on crack growth is apparent.

4. Discussion

Since crack growth in vitreous silica is the consequence of a stress induced chemical reaction between water and siloxane bonds at the crack tip, crack growth behavior can, in principle, be influenced either by modifying the driving force for fracture (local K_I at the crack tip), or by modifying the mechanism of chemical reaction. Because vitreous silica is a simple glass containing virtually no network modifiers, it is likely that any modification of the driving force will only involve the structure of the surface, and hence, the surface forces acting across the two fracture faces. In the following discussion, both surface force generation and modification of the bond breaking reaction by the external environment will be considered.

4.1 Surface Forces

Since surface forces are known to be present when glass surfaces are in close proximity [8] (i.e. separation distance less than ≈100nm), the possibility of these forces affecting crack growth must be addressed. This potential effect of surface forces on fracture was first recognized by Lawn and his colleagues [9-11].

The forces that arise between surfaces that are brought very close together are of three types: dispersion forces resulting from induced dipole-dipole interactions between the atoms of the solid; double layer forces arising from the charges that form on the surface of glass placed in electrolyte solutions; and structural, or entropic forces that are caused by distortions to the structure of the fluid as the surfaces approach separations of < 1 nm [7, 12, 13]. A considerable literature exists on the magnitude and influence of environment on these forces. Most surface force studies in aqueous environments have been conducted on mica [14-18], because mica surfaces can be prepared with atomic flatness and hence can be brought to distances < 0.1 nm for surface force measurement. For mica, the magnitude of the forces as a function of surface separation distance is known in some detail, and as a consequence, the effect of surface forces on crack growth can be estimated readily. Only one set of data has been collected on silica glass [8], so that, for this solid, the forces as a function of separation distance and environment are not well understood .

Of the three surface forces mentioned above, the structural forces have proven to be the strongest in aqueous environments, and consequently, are the most likely to influence crack growth. These forces have been characterized most extensively in near neutral (pH≈5-6) environments. For mica, structural forces have a range of action of approximately 1 nm, and a maximum reported magnitude, when extrapolated to contact, of ≈20 MPa [18]. For glass, the magnitude is less, ≈1 MPa, but the range of the forces is about the same as for the mica [8].

The magnitude of the structural forces depends both on the structure of the interface, and on the composition of the electrolyte adjacent to the interface [14-18]. In mica, the structural forces increase as the concentration of the electrolyte is increased, reaching a maximum value at concentrations of the order of 1 M. These forces arise as a consequence of the structure of the electrolyte and associated adsorbed species on the mica surface. In the narrow confines of the crack tip, the close proximity of the two fracture surfaces prevents both the surface and electrolyte adjacent to the surface from developing the kind of structures that would normally be present for free surfaces in electrolytes. It is doubtful, for example, that hydrated cations, because of their size [7], ≈0.7 nm in bulk solution, have sufficient space to freely penetrate to the crack tip with their hydration cage intact. Similarly, the types of hydration layers that normally build up at free surfaces in aqueous environments [19-20] probably will not form in the

narrow confines of the crack tip. These constraints lead to an increase in the free energy of the surfaces and the fluid immediately adjacent to the surfaces as their spacing is decreased, and hence, to a repulsive force between the two fracture surfaces.

In addition to these structural forces, double layer forces arise as a consequence of electrical charges on the surface of the glass or mica. At their maximum, the double layer forces are at least an order of magnitude smaller than the structural forces just discussed [8, 15], and are unlikely to be important in the present crack propagation studies. Indeed, crack growth studies in electrolytes selected to modify the double layer force on vitreous silica [6] indicated little if any effect of these forces on crack growth in the range of crack velocities and stress intensity factors studied in the present paper. Finally, since Clarke et al. [10] calculated that dispersion forces only influence crack growth in silica glass at low values of K_{Ia} (<0.1 MPa-$m^{1/2}$), dispersion forces are also not expected to be important in the present study. As of our present state of understanding, only the structural forces (or forces stronger than structural forces) are expected to play a role in establishing crack growth behavior in glass. Hence, the data of the present study will only be analyzed in terms of these forces.

For vitreous silica [8], the magnitude of the surface stress, σ, as a function of separation distance, y, is given by the following equation:

$$\sigma = \sigma_o \exp(-2y/D_o) \qquad (1)$$

where σ_o is the stress extrapolated to contact, and D_o is the relaxation distance. Using this equation and following the procedure outlined by Lawn [9], the following equation is obtained for the stress intensity factor resulting from the surface forces:

$$K_\pi = \sigma_o D_o [G/(K_{Ia}(1-\mu))] \qquad (2)$$

The derivation of this equation assumes K_π is considerably less that K_{Ia}. As K_π approaches K_{Ia}, the approximation becomes less valid and when K_π and K_{Ia} are comparable in magnitude, then the method outlined in reference 9 must be used to estimate K_π.

The product, $\sigma_o D_o$, is the work absorbed per unit area of surface in separating the surfaces from contact to infinity [9]. Therefore, $\sigma_o D_o/2$, gives the contribution of the surface forces to the fracture surface energy. If so desired, equation 2 may be expressed in terms of the fracture surface energy [9]. The present form of the equation is retained for comparison with surface force data reported in the literature.

The stress intensity factor, K_I, at the crack tip is determined by both the external applied stresses and the stresses along the crack surface, hence, K_I must be equal to the sum of the stress intensity factor, K_{Ia}, due to the external applied forces, and the stress intensity factor, K_π, due to the surface forces:

$$K_I = K_{Ia} + K_\pi = K_{Ia} + \sigma_o D_o [G/(K_{Ia}(1-\mu))] \qquad (3)$$

Since K_I determines the stresses around the crack tip, it is this parameter that is the driving force for crack growth. Therefore, the velocity of crack growth will be determined uniquely by K_I. If the crack tip reaction is not altered by the external environment (i.e. if the same reactants and activated complex are involved in the reaction), then any shift observed in the v-K_{Ia} plot can be attributed to the effect of the environment on the product $\sigma_o D_o$. Equation 3 indicates that K_I is determined by the magnitude and range of the surface forces, σ_o and D_o, and by the magnitude of the applied stress intensity factor, K_{Ia}. All of the terms on the right hand side of equation 3 can, in principle, be determined experimentally, so that the equation provides a unique relation between K_{Ia} and K_I. When applied to crack growth data, equation 3 can be used to correct K_{Ia} for the presence of surface forces. The slope and position of corrected v-K_I curves are entirely determined from the constants in this equation, i.e. there are no disposable parameters in the final curve.

The magnitude of K_π can be determined for vitreous silica tested in slightly acidic water by substituting appropriate values of σ_o, D_o and the elastic constants into equation 2: μ = 0.21, and G = 28 GPa for vitreous silica. In water, pH≈5, $\sigma_o \approx 1$MPa and $D_o \approx 1$nm giving [8]:

$$K_\pi = 3.54 \times 10^{-5} / K_{Ia} \qquad (4)$$

At the normal values of K_{Ia} used in the present experiment, $K_{Ia} > 0.25$ MPa-$m^{1/2}$, so that $K_\pi < 1.41\ 10^{-4}$ MPa, which is less than 0.1 percent of the applied stress intensity factor in the range used in the present study. This result suggests that, in near neutral environments, surface forces have no great influence on crack motion in vitreous silica. This is an important conclusion, because if it is assumed that surface forces account for the difference in v-K_{Ia} slope between neutral and basic solutions, then the total effect of surface forces on the position of the v-K_{Ia} curves must be attributed to forces that arise in basic solutions.

Based on the assumption that surface forces only affect crack growth in basic solutions, the magnitude of this effect can be estimated from equation 3 and the data in figure 3. First the data in figure 3 are used to obtain a value for $\sigma_o D_o$. This is done by assuming that in neutral solution, $K_I = K_{Ia}$, so that at a given crack velocity the difference between the stress intensity factor in basic solutions and that in neutral solutions is just due to the effect of the surface forces. In this case,

$\sigma_o D_o = (K_I - K_{Ia}) K_{Ia} ((1-\mu)/G)$, where K_{Ia} is the applied stress intensity factor evaluated in the basic solution at the same crack velocity as K_I in the neutral solution. The best fit to the data is obtained if K_I and K_{Ia} are determined at a velocity taken at the centroid of the crack velocity data ($\approx 10^{-6}$m/s). Using equation 3, the effect of surface forces on the v-K_{Ia} curve is estimated by plotting the calculated value of K_{Ia} as a function of crack velocity. A curve obtained by this procedure, figure 8, is seen to pass through the body of experimental data taken in 1 M KOH. Therefore, the supposition that the shift in the position of the v-K_{Ia} is the result of surface forces is not inconsistent with the equation describing this effect.

The value of $\sigma_o D_o$ obtained by this fit, 0.85 J/m^2, provides a relation between σ_o and D_o that has to be satisfied for the surface force assumption to be valid. If the force range D_o is known, then σ_o can be calculated. Furthermore, the value of $\sigma_o D_o$ can be compared with other values of this parameter calculated from force measurements reported in the literature. In figure 9, values of $\sigma_o D_o$ obtained experimentally from surface force measurements on silica and mica in various media have been plotted along with a curve for $\sigma_o D_o = 0.85$. As can be seen, experimental values of $\sigma_o D_o$ for double layer and structural forces are very much less than those needed to explain the present set of v-K_{Ia} data. By contrast, short range forces related to the cohesive bonding of solids do fall close to the curve representing the data from the present experiment. In particular, the data by Breitmeier and Bailey [21], which were

obtained on mica tested in dodecane, suggest that for this material short range ionic forces ($D_o \approx 0.1nm$) between the fracture surfaces are of the correct magnitude to be consistent with the present set of data. When the forces that hold the surface together are of this magnitude and range, the distinction between physical forces between surfaces and chemical forces between atoms may very well lose their distinction, i.e. the two types of forces may very well be describing the same phenomena.

4.2 Chemical Reactions

The position and slope of the $v-K_{Ia}$ curve can also be changed if the chemical reaction that causes crack growth is modified by the surrounding environment. We consider two types of reactions that affect crack growth in vitreous silica. In one, the rupture of siloxane bonds is induced by chemical species that have acidic and basic groups on adjacent sites of the same molecule [1]. The acidic site is usually a mobile hydrogen that can be transferred to the oxygen part of the siloxane bond during the process of bond rupture. The basic site is an electron donor, and simultaneously attaches to the silicon part of the siloxane bond during the chemical reaction. In aqueous environments, the water molecule fills this role, since it has ionizable hydrogen atoms and lone pair electron orbitals on the oxygen that can act as electron donors. In other environments, molecules such as ammonia, hydrazine or methyl alcohol fill this role and cause crack growth [1, 22].

A second reaction mechanism for crack growth involves a nucleophillic attack of hydroxide ions on silicon of the network structure [5, 23]. In basic solutions, hydroxide ions attach to silicon atoms, changing their oxygen coordination from four to five; this has the effect of transferring electrons from the siloxane bond to the adjacent oxygen, thus weakening the siloxane bond. When subjected to an external force, the weakened siloxane bonds either rupture directly, or are hydrolyzed by the water in the environment. This type of reaction is known to be important to the corrosion of glass in basic solutions, pH>9 [5].

The susceptibility of siloxane bonds to attack by either water molecules or hydroxide ions was discussed by Budd [23], who suggested that the activated complex is different for the two reactions. Therefore, it follows that the reaction rate and its dependence on temperature and stress will also be different. In acidic or neutral solutions where the effective concentration of water is high, water molecules will be the primary chemical species to induce crack advance. Conversely, in basic solutions where the hydroxide ion concentration is high, hydroxide ions will be the primary cause of subcritical crack growth.

This suggestion that crack growth in aqueous solutions is caused either by water molecules or by hydroxide ions provides a natural explanation for shifts in the position and slope of the $v-K_{Ia}$ curve. Since the activated species differ for the two reactions, the crack growth curves obtained in acidic and basic solutions will also differ. From reaction rate theory [3, 24-25],

the fact that the slope of the $v\text{-}K_{Ia}$ curve is greater in acids than in bases, suggests a greater activation volume (i.e. a greater strain) for bond rupture in acidic environments. Apparently, the external work that must be put into the rupture of a siloxane bond is greater in acidic than in basic environments.

If the role of water and hydroxide ions in the bond breaking process is accepted, it follows that the influence of cations on crack growth has to result from their effect on either the chemical activity of the water, or the chemical activity of the hydroxide ions in solution. The effect of cation concentration on the activity of water can be measured easily, since this activity is determined from the vapor pressure of water over the solution of interest. Although a decrease in the activity of the water causes a proportional decrease in the crack velocity, it is unlikely that this effect is important, since the vapor pressure of water is about the same for all of the hydroxide solutions used in the present study. At 100°C, for example [26], the vapor pressure of 1 M solutions of LiOH, NaOH and KOH are 722.6, 737.4 and 730.5 torr respectively. This difference in vapor pressure corresponds to a change in chemical activity of only ≈3 to ≈5 percent of that of pure water at this temperature. Since crack velocity is expected to be roughly proportional to the chemical activity of water [3, 25], this change in activity cannot possibly account for the relatively large shifts in the $v\text{-}K_{Ia}$

curve observed in the present paper. Therefore, the main influence of cation on crack growth must result from its effect on the hydroxide ion activity at the reaction site.

In contrast to water, the chemical activity of hydroxide ions in aqueous solutions is strongly affected by the nature of the cation because of the possibility of chemical association between cations and hydroxide ions. To the extent that this happens, the chemical activity of the hydroxide ion in solution is reduced below that expected from complete dissociation of the alkali metal hydroxide. Chemical association of hydroxide ions with alkali metal ions is greatest for lithium ions because of their small size and strong electric field. Association also occurs for sodium ions, but to a much lesser extent, and does not occur at all for potassium or cesium ions. Thus, the dissociation constants for LiOH and NaOH, (pK=-.08 for 0.1 molal LiOH and -.07 for 0.1 molal NaOH [27]), suggest a higher degree of association of Li^+ with OH^-.

To further test the thesis that association effects crack growth, additional crack growth studies were conducted in 1 M KOH saturated with thallium(I) nitrate. Thallium(I) was chosen because it also associates with hydroxide ions and exhibits considerable solubility in basic solutions [26]. As in the case of the equivalent lithium solution, figure 7, the slope and position of the v-K_{Ia} curve differ significantly from that obtained in the 1 M potassium hydroxide solution, figure 10. Thus we have two examples of ions that associate and also affect

crack growth in basic electrolytes. The results of this experiment support the thesis that association plays an important role in the fracture process. Furthermore, the fact that the Li^+ is so much smaller than Tl^+, 0.06 nm versus 0.144 nm, suggests that association and not ion size is the determining factor in the effect of these cations on crack growth.

When vitreous silica is placed in an aqueous solution, the main role of the cations is to compensate the charge that develops at the surface of the silica as a consequence of hydrolysis [5]. This surface charge is determined mainly by the concentration of hydrogen ions in solution. In acidic solutions, pH≈2, the surface of the glass is almost entirely covered with silanol groups so that the surface is virtually uncharged. As the pH is increased, the surface gradually hydrolyzes forming silanolate groups, thus developing a negative surface charge, primarily between a pH of 5 and 11. Therefore, when the pH of the test environment exceeds 11, the surface is fully charged. For electrical neutrality, this surface charge has to be compensated by cations in solution, so that for a pH > 11, the silica surface is completely covered by counter ions. At a free surface, some of these counter ions may be specifically bonded to the surface, while others form a diffuse cloud in the vicinity of the silica surface [20].

At the tip of a crack two of these surfaces with their double layer structure are held in close proximity by the geometry of the crack so that the charge compensating counter ions are also

held in close proximity. In the narrow confines of the crack tip, it is unlikely that a diffuse cloud of counter ions is present, or that the counter ions are fully hydrated[2]. More likely, the counter ions are specifically bonded to the surface with as many water molecules in their vicinity as is possible in the narrow confines of the crack tip. Regardless of the particular details of the crack tip structure, the hydroxide ions must penetrate between this double layer of counter ions to reach the crack tip before they can influence crack growth. As the hydroxide ions pass close to the counter ions, their capture to form alkali metal hydroxide molecules becomes probable, preventing them from reaching the crack tip where they can react. The concentration of hydroxide ions at the crack tip is effectively reduced by this association, and when the decrease in concentration is sufficient, crack advance by hydroxide ion attack will no longer occur. Instead crack advance will be caused by water in solution. In this way, the kinetics of crack growth in 1 M LiOH will be similar to that occurring in water rather than in a highly basic solution.

Alternatively, the associated LiOH molecule may play the same role in the rate limiting step of the reaction as water does in neutral or acidic solutions. Because of the similarity of the structure of LiOH to water, the kinetics of this reaction might be expected to be similar to that occurring in water. In either

case, as the concentration of the LiOH decreases, the degree of chemical association of the LiOH also decreases so that association eventually plays no role in the crack growth process.

Additional evidence that the chemical behavior of lithium differs from that of other alkali metal ions with regard to silica comes from the silica chemistry literature. It has been documented that lithium silicates are much less soluble in bases than silicates of other alkali ions [5], and that high concentrations of lithium (and sodium) ions cause the precipitation of silica in highly basic solutions, whereas potassium and cesium ions do not [28]. Lawrence and Vivian [29] showed that the dissolution of vitreous silica in basic solutions was dependent on the cation used to make up the solution. The reaction of lithium hydroxide with silica differed considerably from that with sodium or potassium hydroxide. Whereas silica dissolves freely in solutions of potassium or sodium hydroxide, dissolution was retarded significantly in solutions of lithium hydroxide. Furthermore, the solubility of silica in lithium hydroxide solutions seemed to decrease as the concentration of the lithium hydroxide was increased. Finally, when lithium hydroxide was present, the dissolution of silica by sodium and potassium hydroxide was greatly retarded. This behavior is similar to that reported for crack growth in our own studies, and suggests that a chemical mechanism may be appropriate to explain the various aspects of the behavior of silica in lithium hydroxide solutions.

Summary

In this paper, crack growth studies were conducted in 0.001 M and 1 M lithium, sodium, potassium and cesium hydroxide solutions to evaluate the effect of cation on the propagation of cracks in vitreous silica. It was observed that only lithium hydroxide in solutions of greater than 1 M had any effect on the crack propagation behavior. The slope and position of the $v-K_{Ia}$ curve for this environment were similar to those obtained in water and in acidic solutions.

The data were analyzed with regard to surface forces acting between the fracture surfaces at the crack tip. Based on the surface force model, an evaluation of the force constants (σ_o and D_o) suggests that double layer forces and structural forces are too weak to explain the experimental crack growth data. Crack growth data are consistent with the idea that the forces necessary to explain the shift in the data in 1 M LiOH must be similar in magnitude and range to the cohesive forces that bind materials together (i.e. high magnitude, ≈3 GPa; short range, ≈0.3 nm). Surface forces of this magnitude have not yet been measured on vitreous silica in basic solutions.

A more likely chemical-based argument to explain the present set of data has also been presented. Fundamental to this argument is the assumption that crack growth in acidic solutions

is a consequence of the reaction of siloxane bonds with water, whereas crack growth in basic solutions is a result of a reaction of these bonds with hydroxide ions in solution. Because lithium ions associate chemically with hydroxide ions, they can bind these ions so that reaction with the crack tip siloxane bonds cannot occur. Other alkali cations do not associate readily with hydroxide ions and hence do not prevent them from reacting at the crack tip. With the hydroxide ions thus removed from the immediate vicinity of the crack tip, crack growth reverts to its behavior in acidic solutions; reaction at the crack tip is primarily with water molecules in solution.

Figure Captions

1. Crack growth data obtained in water (●) and acids (◆) and bases (■). The data for water and the acid lie roughly parallel to one another, whereas the data for the base has a more shallow slope.

2. A comparison of the v-K_{Ia} obtained in 0.001 M solutions of potassium (○) and lithium (●) hydroxide. These data suggest that the effects of cation type on crack growth rate is negligible in solutions of such dilute concentrations.

3. A comparison of crack growth on vitreous silica taken in 1 M KOH (○) and 1 M LiOH (●). As can be seen from figure (a), the effect of cation on crack growth is substantial in these concentrated hydroxide solutions. The curve for the LiOH is essentially identical to that for water (○), figure (b).

4. A comparison of crack growth data obtained in 1 M CsOH (●), and 1 M NaOH (●) with that obtained in 1 M KOH (○) : (a) 1 M NaOH; (b) 1 M CsOH. The data from the KOH solution is essentially identical to those from the other two solutions, indicating little if any effect of cation type on the crack growth behavior.

5. A plot of the crack velocity as a function of LiOH concentration. Results show that crack growth in concentrations of 0.01 M (▲) and 0.1 M LiOH (○) is indistinguishable from that in 0.001 M LiOH (●) solution. Between concentrations of 0.1 M and 1.0 M (△), however, the effect of Li^+ on crack growth is readily apparent. A further decrease in crack velocity is experienced as the solutions approach saturation (≈5 M [26].

6. Effect of lithium ion concentration on crack growth behavior in a Li^+ solution formed by adding a sufficient quantity of $LiNO_3$ to 0.001 M LiOH to bring the total concentration of Li^+ to a concentration of 1 M. The fact that the two sets of data, LiOH (○) and LiOH+$LiNO_3$ (●), overlap indicate little if any effect of lithium ion concentration, by itself, on crack growth behavior. Apparently, Li^+ is effective in modifying the crack growth behavior only if the concentration of OH^- is also high.

7. The effect of 1 M KOH (○) and equal quantities of 1 M KOH and 1 M LiOH (●) on crack growth. The mixed cation solution behaved similarly to that of a 1 M LiOH solution suggesting that when the hydroxide ion concentration of the test environment is high enough, the full effect of the Li^+ on crack growth is apparent.

8. Fit of the $v\text{-}K_{Ia}$ data in figure 1 to equation 3. The calculated $v\text{-}K_{Ia}$ curve passes through most of the body of data collected in 1 M KOH (○), suggesting that the difference in crack growth behavior in LiOH (●) and other alkali metal hydroxide solutions could be based on surface arguments.

9. A comparison of $\sigma_o D_o = 0.85$ with several force measurements reported in the literature. Only measurements in which the force has been reported as a function of surface separation are given above: Structural forces on mica tested in 1 M KCl, Pashley and Israelichvili [18]; Structural and Double-Layer forces on vitreous silica tested in water, Peschel et al. [8]; Ionic forces in mica, Breitmeier and Bailey [21]. In addition, an estimated value of the cohesive strength of glass [30] is plotted assuming a decay distance of 0.3 nm. The data on lecithin is obtained by a non-fracture technique in which the layer spacing is determined as a function of pressure by x-ray diffraction analysis [31].

10. Crack growth studies in 1 M KOH (○) and 1 M KOH saturated with $TlNO_3$ (●). The results are similar to those obtained in the LiOH solutions. As with the lithium hydroxide solutions the slope of the $v\text{-}K_{Ia}$ curve in the concentrated solution is significantly greater than that in the dilute solution.

Footnotes

1. Chemical environments such as ammonia, hydrazine and formamide also cause crack growth in glass [1], but these environments are not considered in this paper.

2. The fully hydrated counter ions are completely surrounded by water and have a diameter of ≈0.7 nm for the alkali metal ions. Depending on the magnitude of K_{Ia}, this diameter can be larger than the displacement of the faces of the crack near the crack tip, so that the hydrated ions would be sterically hindered from reaching charge sites near the crack tip.

References:

1. T.A. Michalske, and S.W. Freiman, "A Molecular Mechanism for Stress Corrosion in Vitreous Silica," J. Am. Ceram. Soc. 66, 284-88 (1983).

2. S.M. Wiederhorn, "Influence of Water Vapor on Crack Propagation in Soda-Lime Glass," J. Am. Ceram. Soc. 50, 407-14 (1967).

3. S.M. Wiederhorn, S.W. Freiman, E.R. Fuller, Jr. and C.J. Simmons, "Effect of Water and other Dielectrics on Crack Growth," J. Mater. Sci. 17, 3460-78 (1982).

4. S.M. Wiederhorn and H. Johnson, "Effect of Electrolyte pH on Crack Propagation in Glass," J. Am. Ceram. Soc. 56, 192-197 (1973).

5. R.K. Iler, The Chemistry of Silica, John Wiley & Sons, New York (1979).

6. S.M. Wiederhorn and H. Johnson, "Effect of Zeta Potential on Crack Propagation in Glass in Aqueous Solutions," J. Am. Ceram. Soc. 58 [7-8], 342 (1975).

7. J.N. Israelachvili, Intermolecular and Surface Forces, Academic Press, New York (1985).

8. G. Peschel, P. Balauschek, M.M. Mller and R. Knig, Colloid and Polymer Science, 260 [4], 444-51 (1982).

9. B.R. Lawn, "Interfacial Forces and the Fundamental Nature of Brittle Cracks," Appl. Phys. Lett. 47 [8], 809-11 (1985).

10. D.R. Clarke, B.R. Lawn and D.H. Roach, "The Role of Surface Forces in Fracture," in Fracture Mechanics of Ceramics, Vol. 7/8, R.C. Bradt, A.G. Evans, D.P.H. Hasselman, and F.F. Lange, eds., Plenum, New York, in press.

11. D.H. Roach, D.M. Heuckeroth and B.R. Lawn, J. Colloid and Interface Sci., in press.

12. J.N. Israelachvili, "The Forces Between Surfaces," Phil. Mag. A43 [3], 753-70 (1981).

13. J.N. Israelachvili, "Forces Between Surfaces in Liquids," 16, 31-47 (1982).

14. J.N. Israelachvili and G.E. Adams, "Measurement of Forces between Two Mica Surfaces in Aqueous Electrolyte Solutions in the Range 0-100 nm," J. Chem. Soc., Faraday Trans. I 74, 975-1001 (1978).

15. R.M. Pashley, "DLVO and Hydration Forces between Mica Surfaces in Li^+, Na^+, K^+ and Cs^+, Electrolyte Solutions: A Correlation of Double-Layer and Hydration Forces with Surface Cation Exchange Properties," J. Colloid Interface Sci. 83 [2], 531-46 (1981).

16. R.M. Pashley and J.N. Israelachvili, "DLVO and Hydration Forces between Mica Surfaces in Mg^{2+}, Ca^{2+}, Sr^{2+} and Ba^{2+} Chloride Solutions," J. Colloid Interface Sci. 97 [2], 446-55 (1984).

17. R.M. Pashley, "Forces between Mica Surfaces in La^{3+} and Cr^{3+} Electrolyte Solutions," J. Colloid Interface Sci. 102 [1], 23-35 (1984).

18. R.M. Pashley and J.N. Israelachvili, "Molecular Layering of Water in Thin Films between Mica Surfaces and its Relation to Hydration Forces," J. Colloid Interface Sci. 101 [2], 511-23 (1984).

19. G.R. Wiese, R.O. James, D.E. Yates and T.W. Healy, "Discreteness of Charge and Solvation Effects in Cation Adsorption at the Oxide/Water Interface," Faraday Society Disc. 52, 302-310 (1971).

20. G.R. Wiese, R.O. James, D.E. Yates and T.W. Healy, pp 54-100 in International Review of Science: Physical Chemistry Series Two, Vol. 6, Electrochemistry, J.O.M. Bockris (ed.), Butterworths, London, 1976.

21. U. Breitmeier and A.I. Bailey, "Interaction Forces between Mica Surfaces at Small Separations in Polar and Non-Polar Liquids," Surface Sci., 89, 191-195 (1979).

22. T.A. Michalske, B.C. Bunker, W.L. Smith and D.M. Haaland, "Reactivity of Strained Surface Sites on Silica," Presented at the 87th Annual Meeting of the American Ceramic Society, May 6, 1985, Cincinnati, OH.

23. S.M. Budd, "The Mechanisms of Chemical Reaction between Silicate Glass and Attacking Agents: Part I. Phys. Chem. Glasses 2 [4], 111-114 (1961).

24. R.J. Charles and W.B. Hillig; pp 511-27 in Symposium on Mechanical Strength of Glass and Ways of Improving It. Florence, Italy, September 25-29, 1961. Union Scientific Continentale du Verre, Charleroi, Belgium (1962).

25. S.M. Wiederhorn, E.R. Fuller, Jr., and R. Thomson, "Micromechanisms of Crack Growth in Ceramics and Glasses in Corrosive Environments," Metal Sci. 14 [8-9], 450-58 (1980).

26. Handbook of Chemistry and Physics, 63rd edition, R.C. Weast and M.J. Astle (ed.), CRC Press, Boca Raton, FL (1982).

27. C.W. Davies, Ion Association, Butterworths, Washington, DC (1962).

28. J. Depasse and A. Watillon, "The Stability of Amorphous Colloidal Silica," J. Colloid Interface Sci. 33 [3], 430-38 (1970).

29. M. Lawrence and H.E. Vivian, "The Reaction of Various Alkalis with Silica," Australian J. Appl. Sci. 12, 96-103 (1961).

30. R.J. Charles, pp 1-38 in Progress in Ceramic Science, Vol. 1, J.E. Burke, ed., Pergamon Press, New York (1961).

31. D.M. LeNeveu, R.P. Rand and V.A. Parsegian, "Measurement of Forces between Lecithin Bilayers," Nature 259, 601-603 (1976).

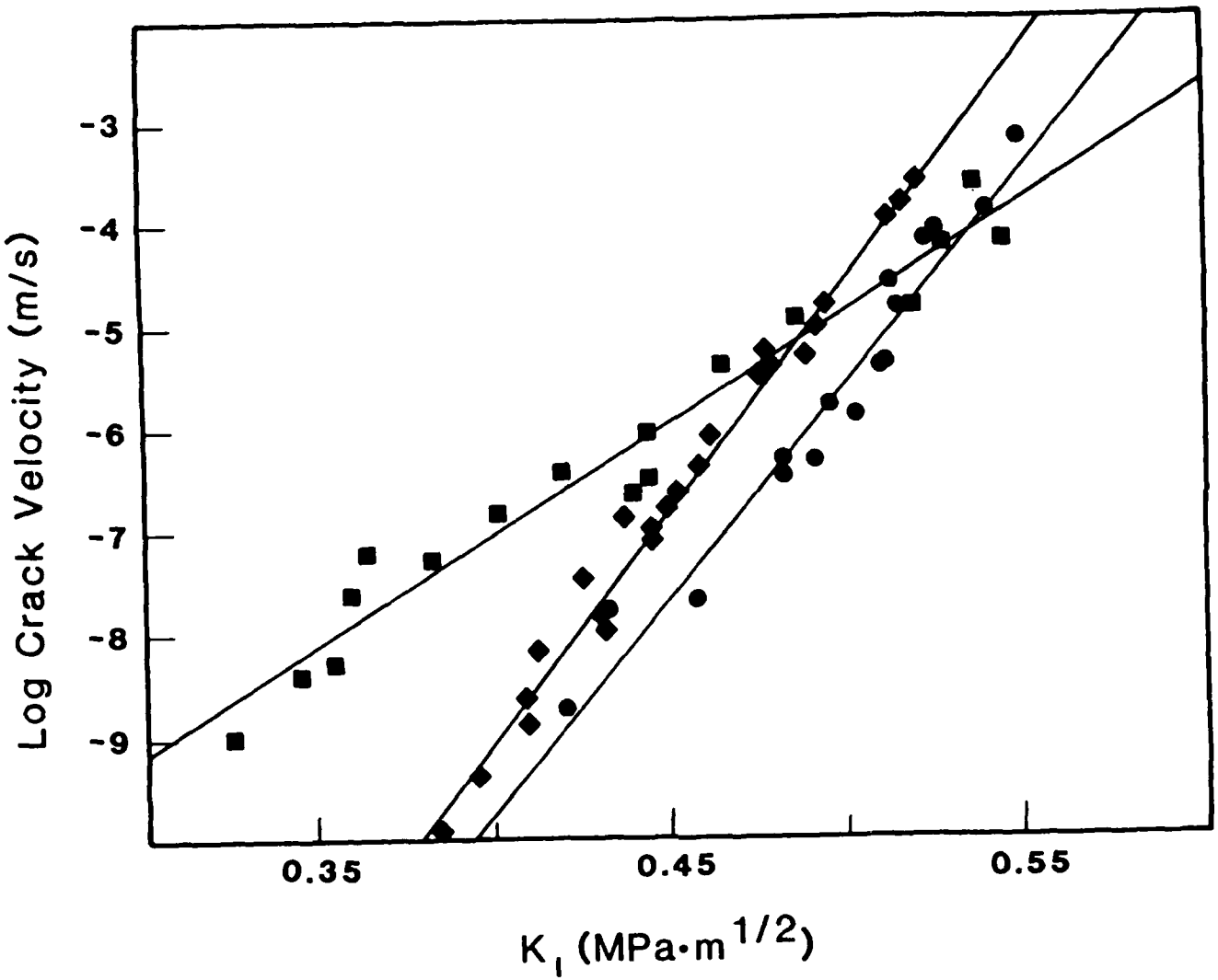
Log Crack Velocity (m/s)
-3
-4
-5
-6
-7
-8
-9
0.35
0.45
0.55
K_I (MPa·m$^{1/2}$)

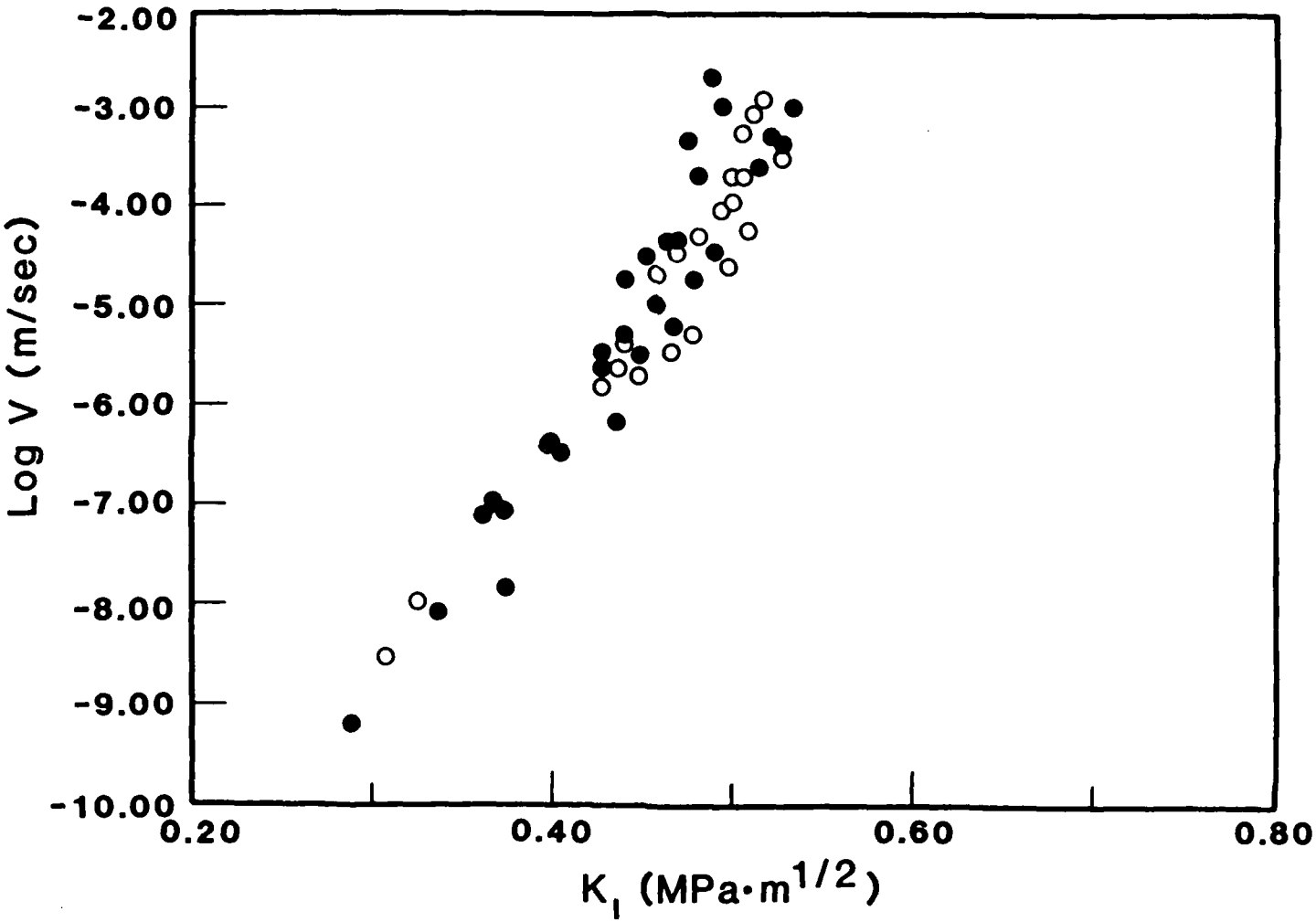
-2.00
-3.00
-4.00
-5.00
-6.00
-7.00
-8.00
-9.00
-10.00
Log V (m/sec)
0.20
0.40
0.60
0.80
K_I (MPa·m^1/2)

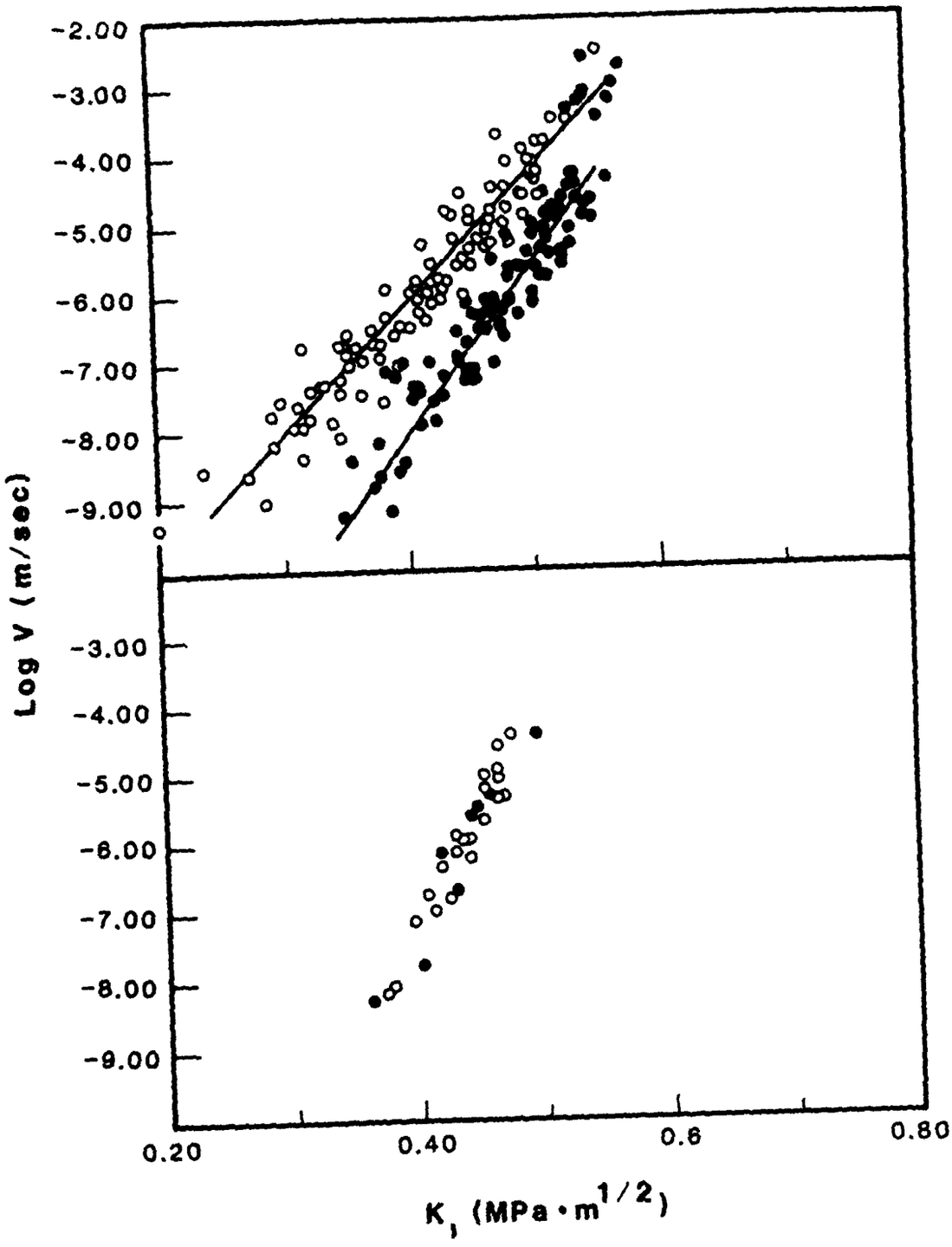
-2.00
-3.00
-4.00
-5.00
-6.00
-7.00
-8.00
-9.00
-3.00
-4.00
-5.00
-6.00
-7.00
-8.00
-9.00
Log V (m/sec)
0.20
0.40
0.6
0.80
K, (MPa • m^1/2)

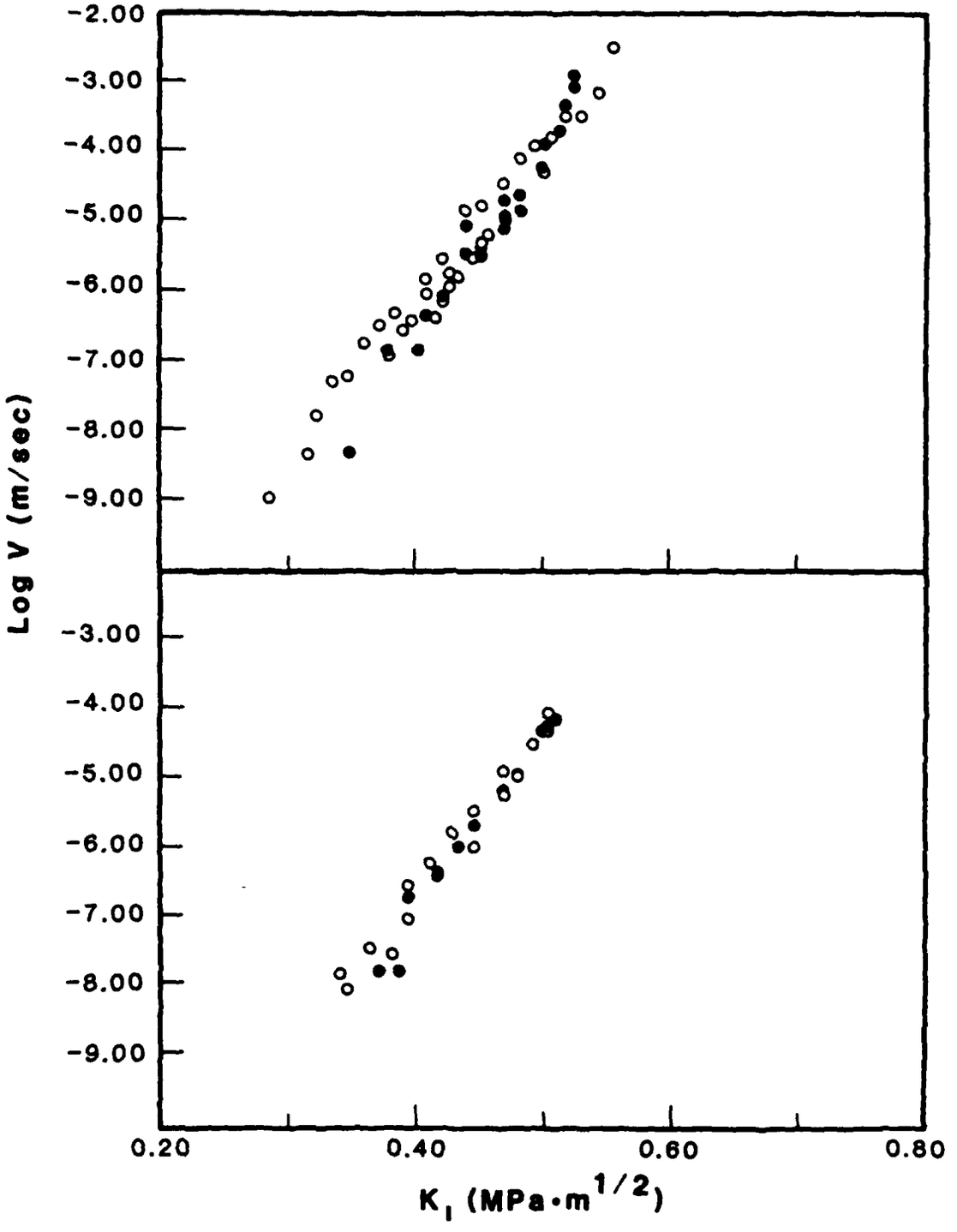
-2.00
-3.00
-4.00
-5.00
-6.00
-7.00
-8.00
-9.00
-3.00
-4.00
-5.00
-6.00
-7.00
-8.00
-9.00
Log V (m/sec)
0.20
0.40
0.60
0.80
K_I (MPa·m^1/2)

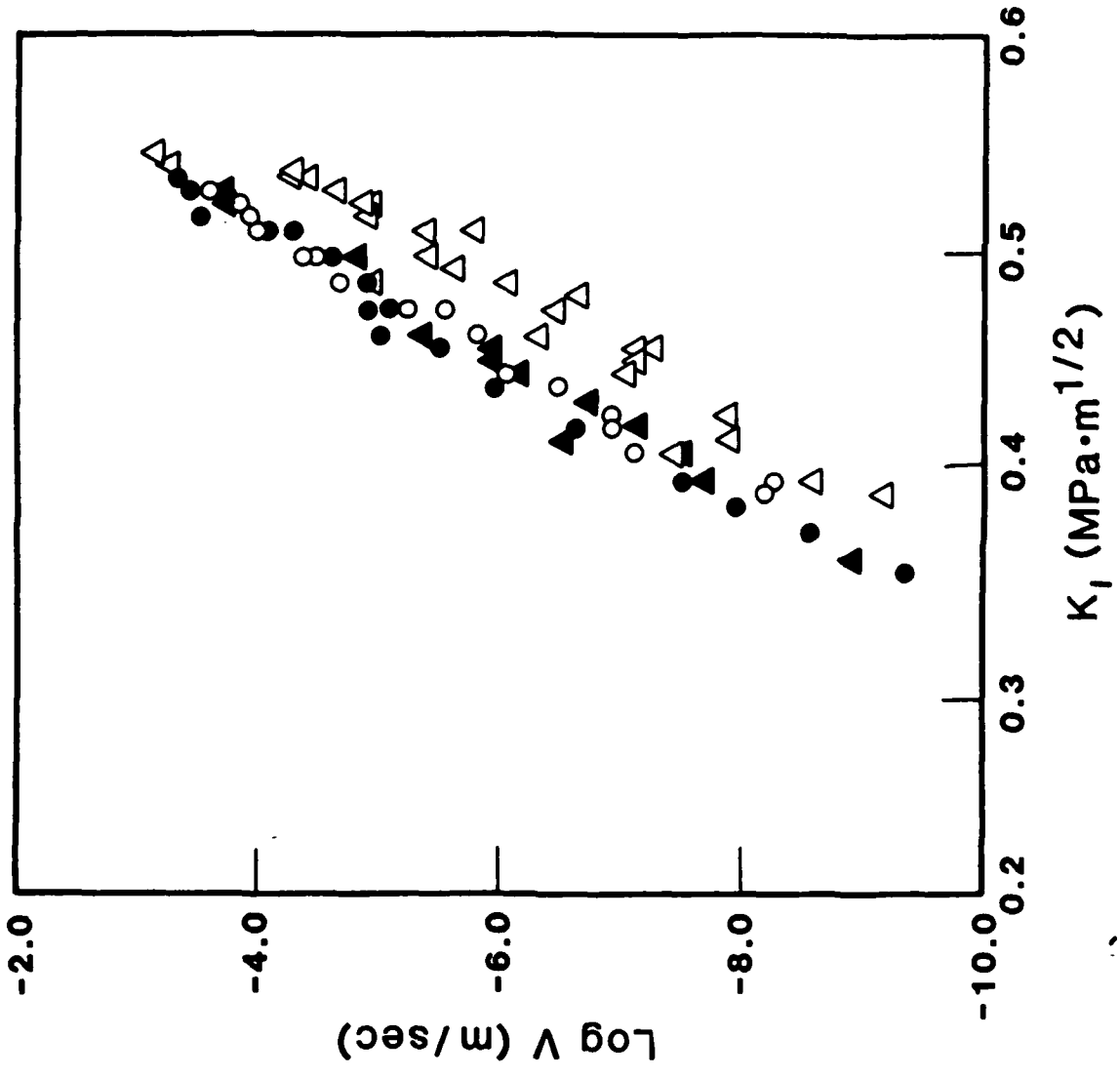
-2.0
-4.0
-6.0
-8.0
-10.0
Log V (m/sec)
0.2
0.3
0.4
0.5
0.6
K_I (MPa·m$^{1/2}$)

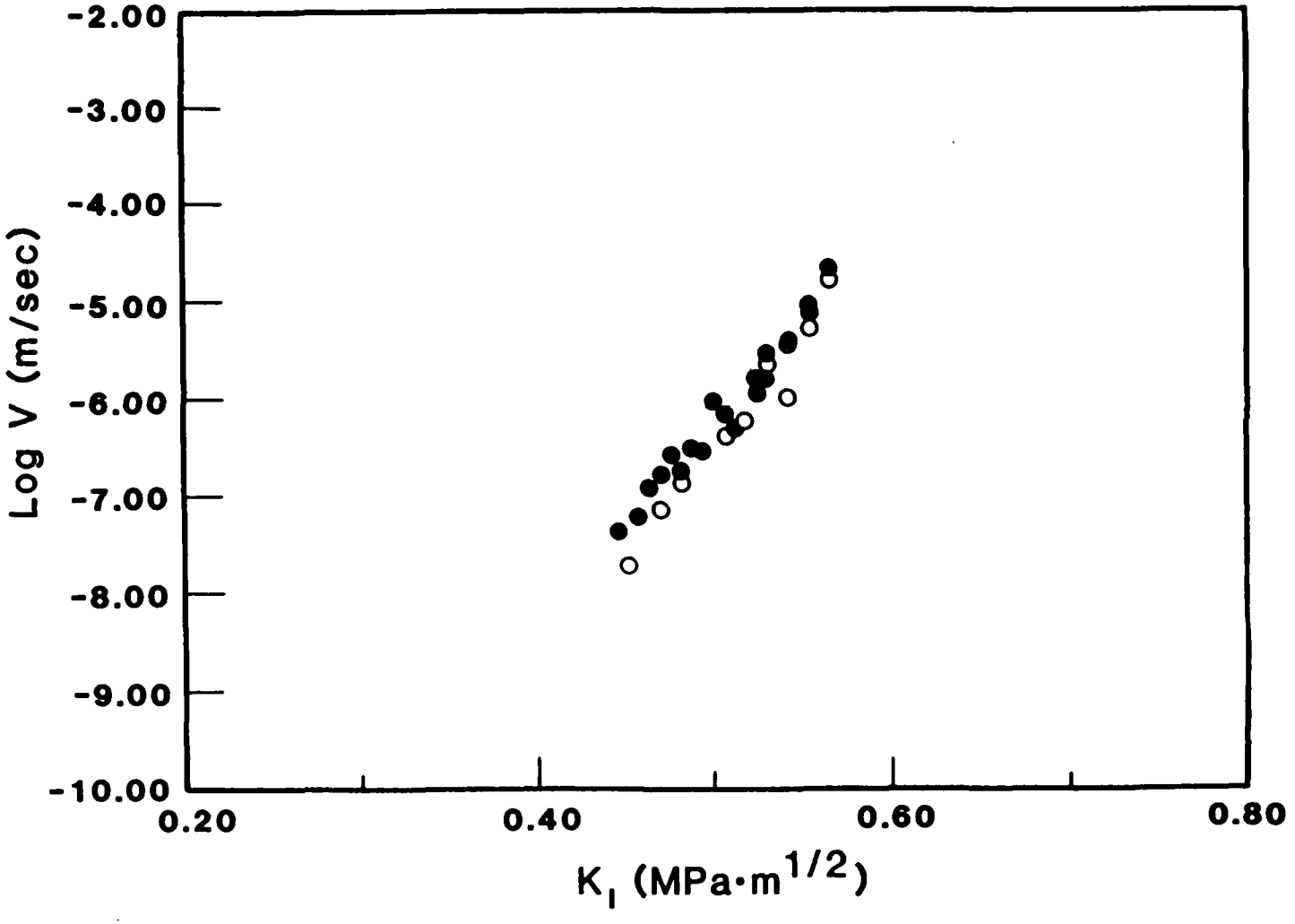
-2.00
-3.00
-4.00
-5.00
-6.00
-7.00
-8.00
-9.00
-10.00
Log V (m/sec)
0.20
0.40
0.60
0.80
K_I (MPa·$m^{1/2}$)

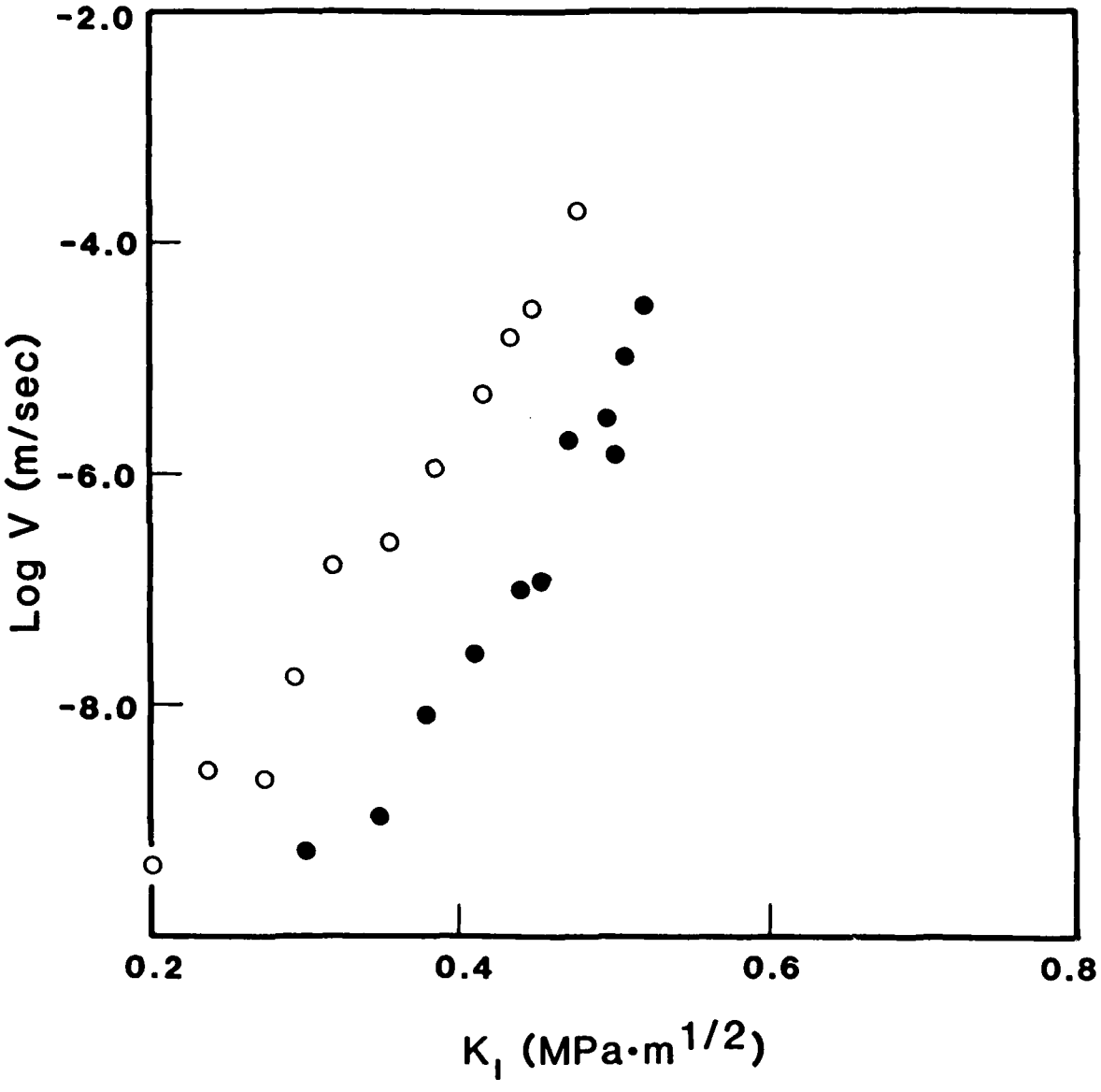
-2.0
-4.0
-6.0
-8.0
Log V (m/sec)
0.2
0.4
0.6
0.8
K_I (MPa·m^1/2)

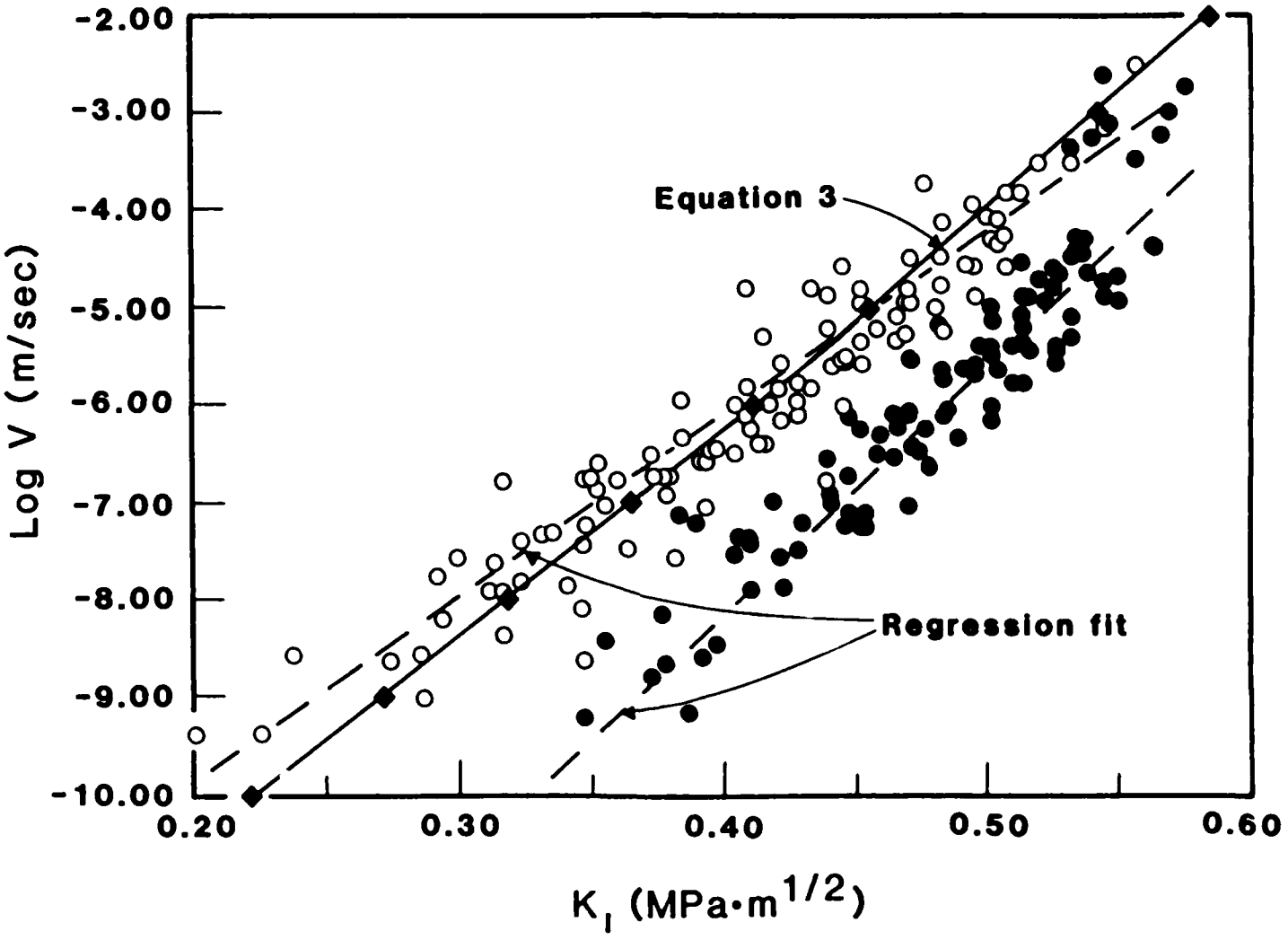
-2.00
-3.00
-4.00
-5.00
-6.00
-7.00
-8.00
-9.00
-10.00
Log V (m/sec)
0.20
0.30
0.40
0.50
0.60
K_I (MPa·$m^{1/2}$)
Equation 3
Regression fit

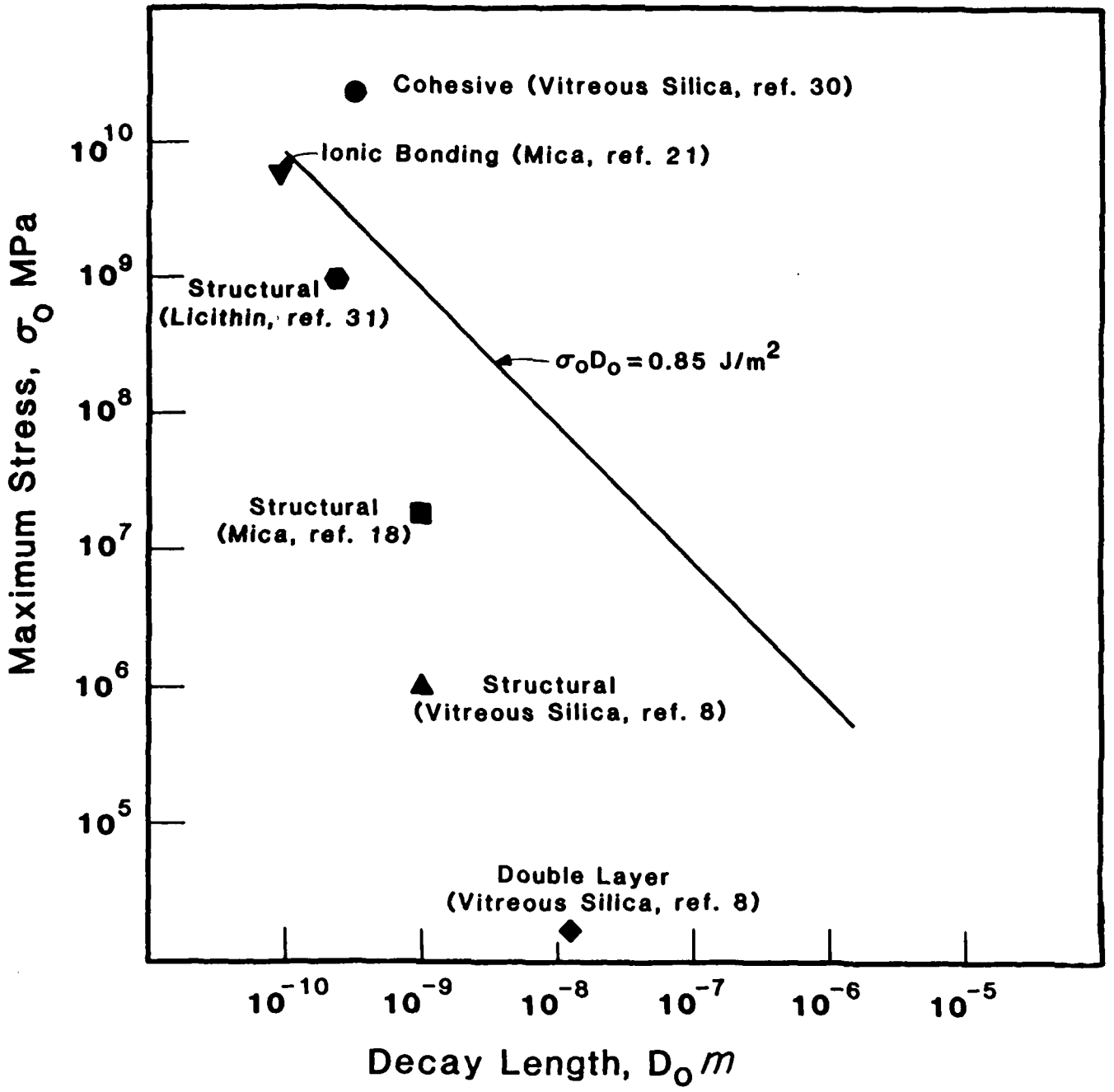
Cohesive (Vitreous Silica, ref. 30)
Ionic Bonding (Mica, ref. 21)
Structural
(Licithin, ref. 31)
$\sigma_o D_o = 0.85$ J/m^2
Structural
(Mica, ref. 18)
Structural
(Vitreous Silica, ref. 8)
Double Layer
(Vitreous Silica, ref. 8)
Maximum Stress, σ_o MPa
10^{10}
10^9
10^8
10^7
10^6
10^5
10^{-10}
10^{-9}
10^{-8}
10^{-7}
10^{-6}
10^{-5}
Decay Length, D_o m

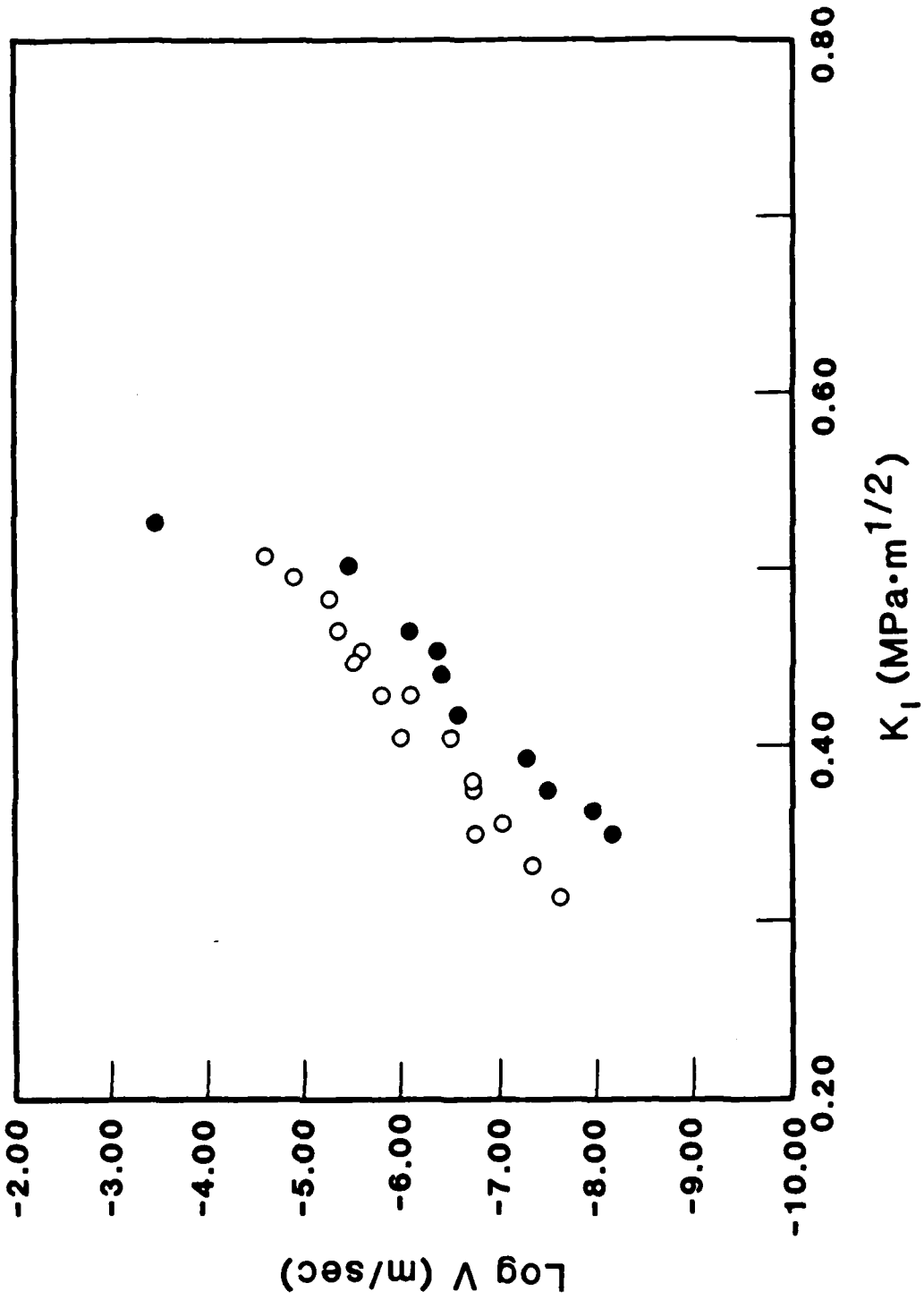
Log V (m/sec)
-2.00
-3.00
-4.00
-5.00
-6.00
-7.00
-8.00
-9.00
-10.00
0.20
0.40
0.60
0.80
K_I (MPa·m$^{1/2}$)

FRACTURE MECHANISMS IN LEAD ZIRCONATE TITANATE CERAMICS

S.W. Freiman and L. Chuck
National Bureau of Standards
Gaithersburg, MD 20899

J.J. Mecholsky and D.L. Shelleman
Penn State University
University Park, PA 16802

L.J. Storz
Sandia National Laboratories
Albuqueque, NM 81785

ABSTRACT

Lead Zirconate Titanate (PZT) ceramics can be formed over a wide range of $PbTiO_3/PbZrO_3$ ratios and exist in a number of crystal structures. This study involved the use of various fracture mechanics techniques to determine critical fracture toughness, K_{IC}, as a function of composition, microstructure, temperature, and electrical and thermal history. The results of these experiments indicate that variations in K_{IC} are related to phase transformations in the material as well as to other toughening mechanisms such as twinning and microcracking.

In addition, the strength and fracture toughness of selected PZT ceramics were determined using specimens in which a crack was introduced by a Vicker's hardness indentor. The variation of K_{IC} with composition and microstructure was related to the extent of twin-crack interaction. Comparison of the strength as a function of indentation load with that predicted from indentation fracture models indicates the presence of internal stresses which contribute to failure. The magnitude of these internal stresses has been correlated with electrical properties of the ceramic. Fractographic analysis was used to determine the magnitude of internal stresses in specimens failing from "natural flaws."

INTRODUCTION

Lead-zirconate-titanate (PZT) is a series of solid solutions of $PbZrO_3$ with $PbTiO_3$ as shown in the phase diagram given in Figure 1[1]. The material below the Curie point can exist in a number of crystal structures as designated on the diagram, of which the phases designated F_T (tetragonal), F_R (HT), and F_R (LT) (both rhombohedral) are ferroelectric (FE), and that designated A_O (orthorhombic) is antiferroelectric (AFE). In this paper, we will show that in addition to the fracture mechanisms such as twinning and microcracking which have been identified for another ferroelectric ceramic,

$BaTiO_3$ [2-4], there are additional factors such as the morphotropic phase changes which can contribute directly to fracture. We will show that the concept of "internal stresses" which has been discussed with relation to the fracture of $BaTiO_3$ [2-4], will be broadened to include the possibility of generalized microstructure crack interactions. In addition, a correlation will be established between internal stresses as measured through the electrical characteristics of the material, e.g. polarization loops, and those inferred from the strength measurements.

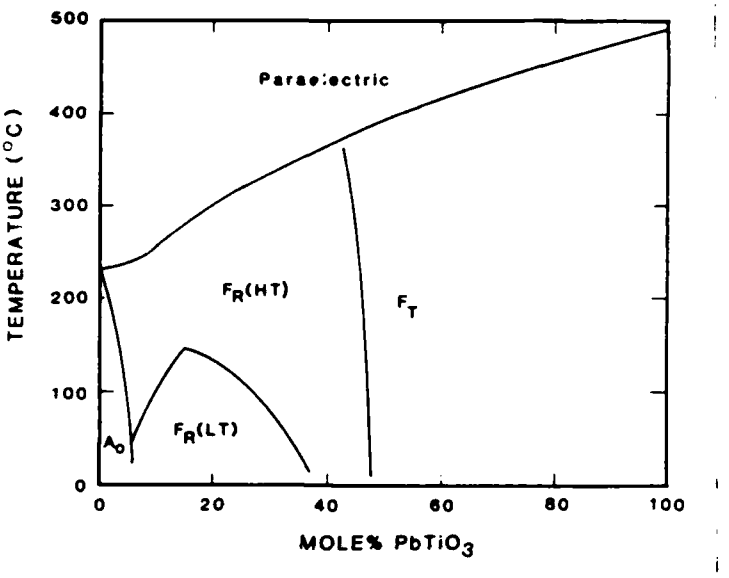

Figure 1. $PbZrO_3$-$PbTiO_3$ phase diagram (after Jaffe, Cook, and Jaffe[1]).

EXPERIMENTAL PROCEDURES

Materials

The PZT materials tested were obtained from a wide variety of sources (Honeywell, Inc.; Sandia National Laboratories; Motorola, Inc.; Nippon Electric; and Plessey, Inc.) The materials were obtained and tested over approximately a ten year period. Although the variability in processing conditions most likely has an effect on the mechanical properties, it is not possible to quantify this relationship. We will show later that controlled composition variations in 95% $PbZrO_3$-5% $PbTiO_3$ (95/5 PZT) can have a significant effect on the fracture process.

The 95/5 PZT materials used in this study were prepared at Sandia National Laboratories from various sources of PbO, ZrO_2, and TiO_2 powders, plus ~ 0.8 wt.% NB_2O_5. The powders were mixed then calcined at 1000 °C. The ceramic billets were bisque fired at 600 °C for 4 hours then sintered at 1310 °C for 6 hours. The grain size of the fired material was in the range of 5-10 μm for most compositions examined, but some specimens were processed to yield smaller grains, 1-2 μm, as well as larger, ~ 100 μm. Fracture toughness data was taken on material in the as-fired condition, after electrical poling at 100 °C at a field of 2000 volts/mm, and after the poled specimens had been hydrostatically depoled at room temperature (pressure ~ 27.6 MPa).

Strength-Fracture Toughness

Most of the critical fracture toughness data reported herein were obtained using the applied-moment-double catilever beam technique[5]. Specimens were nominally 13 x 2 x 40 mm with an ~ 0.5 mm deep groove cut longitudinally down the specimen to guide the crack. A 14 mm long tapered notch was cut into the top of the specimen as a crack initiator. Prior experience indicates that such a notch yields data equivalent to having an actual crack in the specimen. The data was generally obtained by loading the specimen in air or Fluorinert, FC-77, at a rapid crosshead rate (~ 0.5 cm/min) on a universal testing machine. Lower temperature tests were performed in Fluorinert which was cooled by the addition of dry ice to the liquid.

Values of fracture toughness were also obtained on the 95/5 compositions using the indentation-strength procedure described by Chantikul et al.[6] Tests were performed on bars nominally 3 mm x 3 mm x 25 mm. A 15 μm diamond final surface finish on the test bars was used in order to eliminate any surface stresses that may have resulted from specimen preparation. After polishing, the specimens were annealed at 250 °C in air. The indentation was placed in the center of the width of the bar using a Vickers indentor at a range of loads, P. A drop of silicone oil was placed on the indentation site to reduce the tendency for slow crack growth. The bars were broken in 3-point flexure (span 19.4 mm) at a crosshead rate of 0.5 mm/min. The specimens were carefully examined after fracture; only those which had clearly failed from the indentation site were analyzed for K_{IC}. K_{IC} was calculated from the portion of the log σ-log P curve which obeyed the relationship predicted from the indentation model. Deviations from this behavior are discussed later in terms of crack-microstructure interactions.

Fractography

Fractographic analysis of the 95/5 PZT specimens failing from "natural flaws", i.e. pores or machining induced defects), was carried out in the scanning electron microscope. Based on the observed flaw sizes and the critical fracture toughness, K_{IC}, determined independently, the level of "internal stress" was calculated and compared to that determined from indentation-strength studies. General fracture morphologies were determined to establish the ratio of intergranular to transgranular failure as a function of PZT composition.

RESULTS AND DISCUSSION

The fracture behavior of PZT will be discussed in two parts. In the first portion, we will discuss effects of general compositional variations in the PZT system on fracture, particularly fracture toughness. The second part of this section will center on a discussion of the fracture mechanisms important to a specific PZT composition; namely, 95% $PbZrO_3$-5% $PbTiO_3$.

General Compositional Effects; K_{IC}

The critical fracture toughness, K_{IC}, of PZT as measured by an applied moment DCB technique is shown in Figure 2 for material having a range of Zr/Ti ratios. The data can be viewed as passing through a series of maxima and minima in K_{IC}. There is a distinct minimum at the morphotropic boundary between the tetragonal and rhombohedral phases. The minimum at the tetragonal-rhombohedral boundary can be observed even though the data came from various materials prepared at different laboratories using three different techniques. Somewhat less well documented minima occur at the other two phase boundaries in the $PbZrO_3$-$PbTiO_3$ system (Figure 1). Previous work[2,3] has

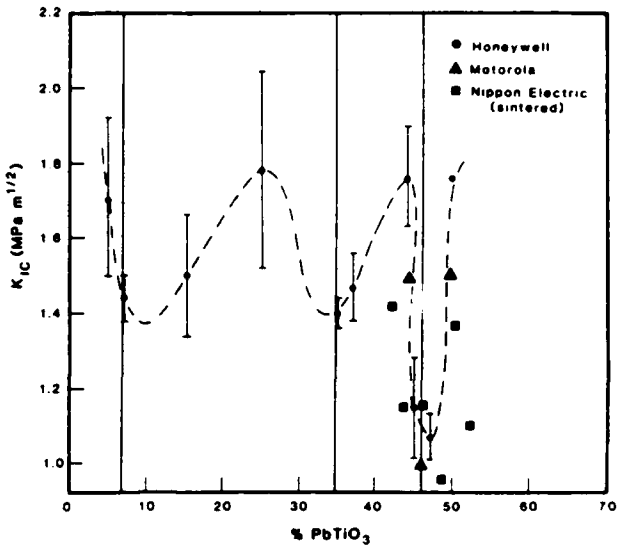

Figure 2. Critical fracture toughness, K_{IC}, as a function of composition in the $PbZrO_3$-$PbTiO_3$ system. Vertical lines indicate the position of the phase boundaries (25 °C) shown in Figure 1.

demonstrated that both crack-twin interactions and microcracking make important contributions to fracture toughness of $BaTiO_3$ in the ferroelectric (tetragonal) state. Neither of these mechanisms are applicable to $BaTiO_3$ in the paraelectric (cubic) state, and therefore a much lower K_{IC} is observed. The fact that the K_{IC} of a commercial PZT* goes from 0.31 MPa $m^{1/2}$ in the cubic state to 0.83 MPa $m^{1/2}$ in the ferroelectric state implies that twinning is important to the toughening process in this material. Further evidence of twinning effects on K_{IC} will be shown later in the discussion on 95/5 PZT.

The data in Figure 2 is in basic agreement with the work of Igarashi and Okazaki[7] who showed that both strength and fracture toughness, as determined by an indentation procedure, pass through a minimum at a Pb/Zr ratio of ~ 46.5/53.5, i.e., the morphotropic boundary. Igarashi and Okazaki also observed that as the Ti concentration was extended beyond the morphotropic boundary it became increasingly difficult to measure the size of the indentation cracks because of a damaged (microcracked) region surrounding the indentation site. They interpreted this damage (microcracking) as being due to internal stresses produced by the increasing distortions of the tetragonal lattice as composition shifts closer to the $PbTiO_3$ end of the phase diagram. These distortions, leading to microcracking, can enhance K_{IC} in direct analogy to effects in $BaTiO_3$. One can calculate the effects of microcracking on trends of K_{IC} with composition in the tetragonal phase regime, following the models developed for Al_2O_3 et al.[8] and $BaTiO_3$ [3]. Rice and Freiman[8] showed that when microcracking is a major source of toughening, the fracture energy γ (= $K_{IC}^2/2E$) can be calculated from the following expression:

$$\gamma = \gamma_p \left(1 - \frac{G}{G_s}\right) + M\overline{\Delta\varepsilon}\left[(9E\gamma_B G)^{1/2} - \overline{\Delta\varepsilon}\, EG\right] \qquad (1)$$

*TLZ-H, Plessey Corporation, Australia

where γ_p is the fracture energy due to all contributions other than microcracking, i.e. intrinsic plus twinning effects, G is the grain size, G_s is the grain size at which spontaneous failure occurs, $\overline{\Delta\varepsilon}$ is the average strain in the lattice, γ_B is the grain boundary (or single crystal) fracture energy, E is Young's modulus, and M is an empirical constant related to the number of microcracks formed at the crack tip. The PZT composition at which the maximum contribution of microcracking to toughness will occur can be determined. By differentiating Equation (1) with respect to $\overline{\Delta\varepsilon}$, and setting the result equal to zero:

$$\overline{\Delta\varepsilon}_m = \frac{1.5M\gamma_B^{1/2}}{(EG)^{1/2}} \qquad (2)$$

Taking M = 2.5 [8], E = 81 GPa, γ_B = 1 J/m^2 [9], and G = 5 μm yields a value for $\overline{\Delta\varepsilon}_m$ = 0.003. This value of $\overline{\Delta\varepsilon}_m$ is smaller than the distortions which occur in the tetragonal lattice, because a portion of the strain is relieved by twinning[2]. Nevertheless, these calculations imply that the toughness of PZT will be maximized at some intermediate composition in the tetragonal phase-field in agreement with the results of Igarashi and Okazaki[7].

Based upon the above discussion, it can be concluded that the maxima and minima in toughness observed in PZT are due to a trade-off between contributions due to twinning and microcracking. At a phase boundary, twin motion is facilitated, making a somewhat higher energy contribution to this toughening mechanism. However, because of reduced internal strain, the degree of microcracking and therefore its effect on K_{IC} will be significantly reduced. Conversely, the maxima in the K_{IC}-composition diagram represent materials in which the contribution of microcracking to toughness is a maximum. Because microcracking is a more effective toughening mechanism than twinning (as observed in $BaTiO_3$ [3]) the overall toughness reflects its contribution to K_{IC}.

95/5 PZT

Detailed studies of the direct effect of PZT microstructure on both strength and fracture toughness were conducted on 95/5 PZT. This composition is located just to the ferroelectric side of the ferroelectric/antiferroelectric phase boundary shown in Figure 1. The material can be driven into the antiferroelectric state by the application of hydrostatic pressure, yielding a simultaneous release of current. Upon release of the pressure, most of the material returns to its original ferroelectric state, although there is a hysteresis in the pressure-temperature diagram[10] (Figure 3) indicating that there are vestiges of AFE domains remaining after pressure release. We will present evidence that these remaining AFE domains can transform to the FE phase at the crack tip, raising the K_{IC} values above those due to twin-crack interactions or microcracking effects.

The critical fracture toughness of 95/5 PZT is shown in Figure 4 for material in the as-fired, electrically poled, and pressure depoled conditions. The pressure depoled material shows an approximately 50% increase in K_{IC} for all grain sizes than those specimens in the as-fired and poled states. Also, if one assumes that microcracking plays a major part in the toughness behavior, Equation (1) can be used to calculate the grain size at which K_{IC} will be a maximum[3]. The curve obtained from Equation (1) is shown in Figure 4 indicating an expected K_{IC} maximum at a grain size of approximately 40 μm. However, experiments are needed to verify this prediction.

K_{IC} is shown as a function of test temperature for a particular 95/5 composition (≈ 10 μm grain size) in both the poled and pressure depoled condition (Figure 5). The pressure depoled material has a higher toughness over the entire temperature range down to approximately -65 °C where it has

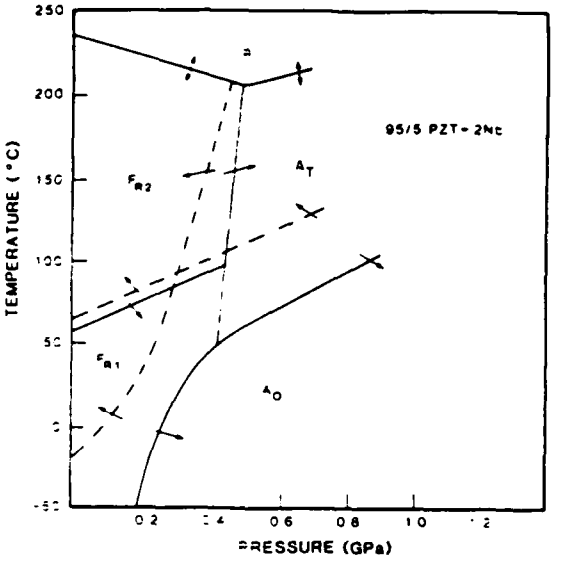

Figure 3. Pressure-temperature phase diagram for 95/5 PZT showing hysteresis in antiferroelectric (A_O) to ferroelectric (F_{R1}) transition (dashed line) as depoling pressure is removed (after Fritz and Keck[10]). The position of the F_{R1} to A_O transition line is very sensitive to composition, which explains the much smaller depoling pressure required for the materials studied herein compared to that in the diagram.

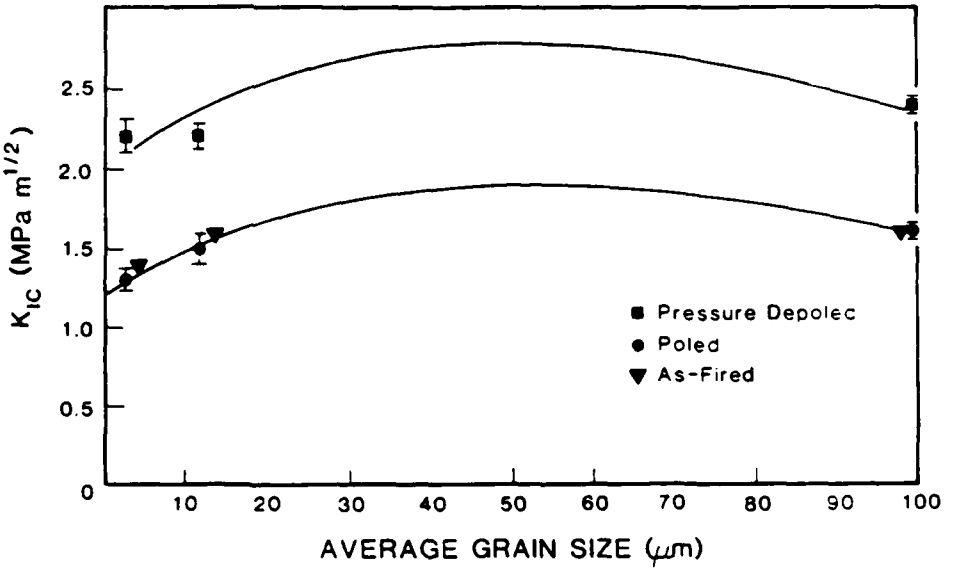

Figure 4. K_{IC} as a function of grain size for a 95/5 PZT after various electrical pretreatments. Curve was drawn to reflect predictions of model for microcracking enhanced toughness[8].

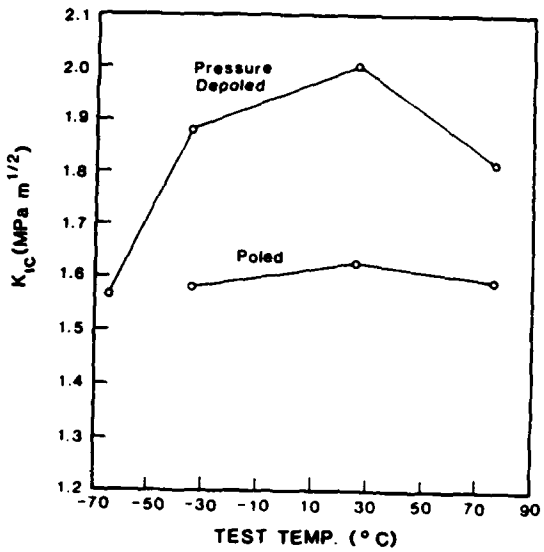

Figure 5. K_{IC} as a function of testing temperature for a 95/5 PZT.

declined sharply. Because twins are present in both the poled and pressure depoled material, a twin-crack mechanism cannot explain this observation. Microcracking probably does contribute somewhat to the toughness, but would not be expected to produce a decrease in K_{IC} at low temperature. We therefore interpret the K_{IC}-temperature behavior in terms of the hysteresis in the antiferroelectric to ferroelectric phase transformation shown in the pressure-temperature-phase diagram for 95/5 PZT (Figure 3). The position of the $A_O \rightarrow F_R$ boundaries for the FE to AFE (solid line) and AFE to FE (dashed line) in Figure 3 show an extensive hysteresis. The AFE → FE transformation after the removal of the hydrostatic depoling pressure becomes more difficult as the temperature is lowered, and requires a negative pressure (tensile stress) below -30 °C. We hypothesize that the transformation of residual AFE domains to FE in the crack tip stress field leads to toughening, in analogy with the mechanism proposed for transformation toughened ZrO_2. Spears[11] has demonstrated remnant AFE phase through electrical measurements, and Kuroda and Heuer[12] have shown the presence of antiferroelectric domains in a pressure depoled material, through the use of transmission electron microscopy. We further hypothesize that the increased barrier to the phase transformation as the temperature is lowered decreases its contribution to toughening. If our hypothesis regarding phase transformation toughening is true, then we should be able to optimize the size and volume fraction of transforming phase. Thus, it is important to continue work to better understand this mechanism of toughening in PZT.

A portion of the study conducted on 95/5 PZT involved a determination of the effect of stoichiometry on fracture toughness and strength. The lead content in the compound $Pb_yNbO_{0.02}(Zr_{0.96}Ti_{0.04})_{0.98}O_3$ was varied from y = 0.96 to 1.02. The material was tested as described in the Experimental Procedure section.

The indentation-strength data obtained from three PZT compositions (y = 0.96, 0.98 (stoichiometric), and 1.01) is shown in Figure 6. The data was analyzed according to Equation (3)[8]:

$$K_c = \eta_v (E/H)^{1/8} (\sigma P^{1/3})^{3/4} \qquad (3)$$

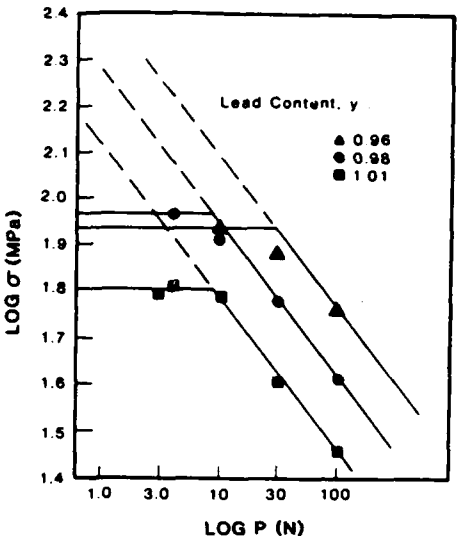

Figure 6. Log fracture stress versus log indentation load, P, for 95/5 compositions. $Pb_yNb_{0.02}(Zr_{0.96}Ti_{0.04})_{0.98}O_3$. Based on indentation model[6], lines of slope -1/3 were drawn through points indented at 100N. Horizontal lines represent strength plateaus observed at small P.

where E is elastic modulus, H is hardness, σ is the fracture strength of bars indented at load, P, and η_v is an empirical constant determined to be equal to 0.59 [8]. The dashed lines in Figure 6 were drawn with slope = -1/3 through the data for large load P. From the position of these curves, a value of K_{IC} can be calculated according to Equation (3). Such calculations yield the values of K_{IC} for the three materials shown in Table 1. The toughest material in terms of resistance to macroscopic crack growth is that with the lowest lead content. This is also the composition in which the highest ratio of transgranular to intergranular failure is observed (Figure 7) and therefore the composition in which the most twin-crack interaction will take place. As in $BaTiO_3$ [2], this twin-crack interaction is a fundamental mode of toughening of PZT in the ferroelectric state. Comparison of indentation-fracture data at room temperature and 250 °C yielded a ratio of K_{IC}(25 °C)/K_{IC}(250 °C) = 2.2, for a 95/5 material, similar to that discussed earlier for a commercial PZT composition near the morphotropic boundary.

In addition to having a direct correlation to fracture toughness, the transformation of both $BaTiO_3$ and PZT from the cubic to the ferroelectric state can also produce local microstructural stresses which can combine with applied stresses to cause mechanical failure. The effect of these stresses on fracture have been demonstrated in $BaTiO_3$ through the use of indentation-fracture procedures[4]. As shown in Figure 6, (for clarity, only three of the six curves obtained are included) the deviation of the data from the $P^{-1/3}$ curve at small indentation loads can be ascribed to the direct effect of microstructural stresses on flaw extension. The different compositions were ranked according to their microstructural effect on strength by plotting $\sigma_{plateau}/\sigma_{(P=100N)}$ as a function of stoichiometry (Figure 8), where $\sigma_{(P=100N)}$ is used as normalizing factor to account for shifts in macroscopic fracture toughness. The largest effect of microstructure was found to occur at the greatest deviations from stoichiometry. While it is still believed that it is the internal stresses in the material which add directly to the applied stress, other phenomena such as increasing K_{IC} with increasing flaw size,

Table 1

FRACTURE TOUGHNESS AND INTERNAL STRESS FOR 95/5 PZT's

Lead Content	Failure Stress (MPa)	K_{IC}(MPam$^{1/2}$)*	Effective Internal Stress (MPa) **
0.96	75 ± 3	1.7	20±3
0.98	74 ±10	1.3	13.5 ± 0.6
1.01	45.7 ± 0.1	1.1	25 ± 1

* From indentation-strength measurements

** Calculated from $\langle \sigma_I \rangle = \sigma_{failure} - \frac{0.8\ K_{IC}}{C^{1/2}}$ (C = flaw size)

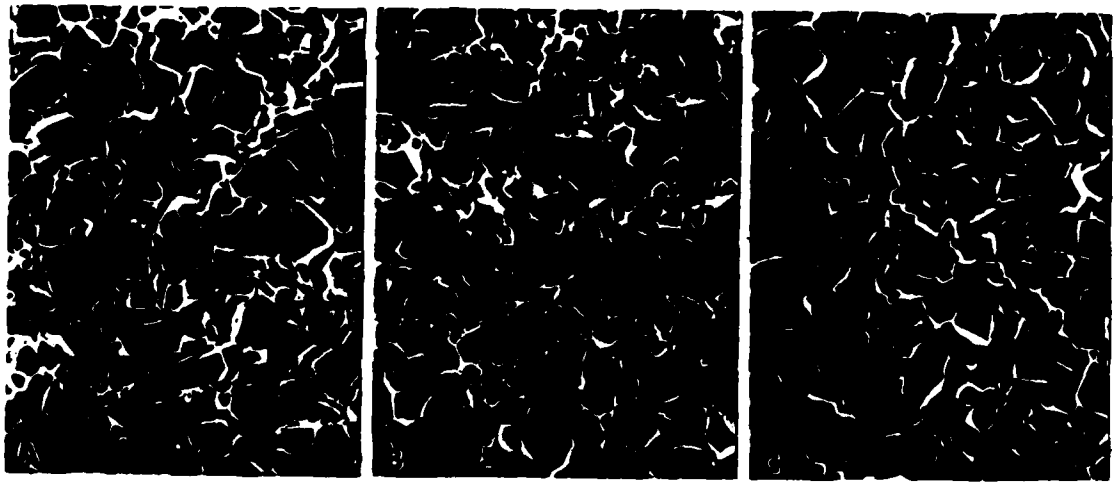

Figure 7. Scanning electron micrographs of fracture surfaces of 95/5 specimens showing variation in ratio of transgranular to intergranular failure. (A) Pb content, y = 0.96; (B) y = 0.98; (C) y = 1.01. Note indications of twin-crack interaction on larger grain faces in (A) and (B).

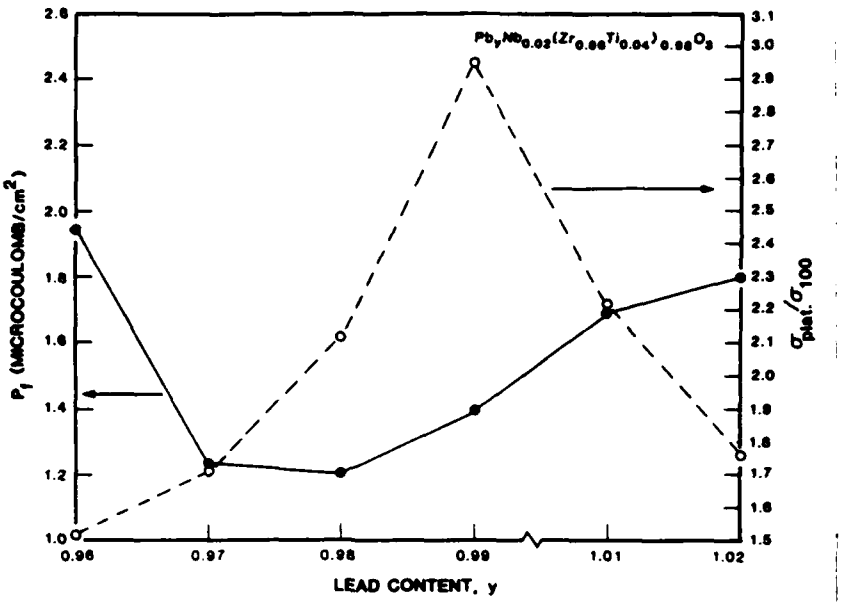

Figure 8. Both level of the strength plateau (Figure 6) and asymmetry of the electrical polarization loops, P_f, for 95/5 PZT as a function of stoichiometry. Strength maximum at approximately the point of smallest loop asymmetry is interpreted in terms of a minimum in the internal stress level.

i.e. "R" curve behavior cannot be ruled out. From a practical viewpoint, these data suggest that the optimum material for use in an actual device would be one near stoichiometry even though the critical fracture toughness is not a maximum here.

Fractographic analysis was performed on failures which occurred from "natural" flaws, i.e., flaws not generated by the Vicker's indentation. Using an expression developed to explain failure in $BaTiO_3$ [2], it was possible to calculate internal stress levels in the three 95/5 PZT materials from K_{IC}, flaw sizes, and strength. These calculations (Table 1) indicate that the levels of internal stress follow the same ranking as the microstructural effect shown by the plateau in the strength.

A correlation has also been obtained between the asymmetry of the electrical polarization curves for these PZT compositions[13] and the level of internal stress. The more asymmetric is the polarization, the greater is the predicted value of stress in the material[13]. The asymmetry of the polarization loops for 95/5 PZT (Figure 8) is seen to be a minimum at essentially the same compositions at which the microstructure has the least effect on strength, i.e. the largest value of $\sigma_{plateau}/\sigma_{(P=100N)}$.

SUMMARY

Fracture in PZT is shown to be a complex process. The resistance of this material to crack growth is dependent on both its chemical composition and microstructure. The competition between toughening due to twin-crack interactions and that due to microcracking is hypothesized to be responsible for the maxima and minima in the K_{IC}-composition plot for PZT. Easier twin motion at the phase boundaries and concomitant reduction in stress levels leading to less microcracking induced toughening is responsible for the minimum in K_{IC} at the morphotropic boundaries. Detailed studies carried out on a

95/5 PZT indicate that in addition to microcracking and twinning the phase transformation from an antiferroelectric to a ferroelectric phase at the crack tip also makes a significant contribution to fracture toughness.

It was shown that indentation-fracture techniques can be used to separate effects of microstructure on toughening and strength. Indentation-fracture data obtained on 95/5 materials demonstrated that K_{IC} is a maximum at the stoichiometric composition and that internal stresses generated by the paraelectric to ferroelectric phase transformation contribute directly to a reduction in the measured strength. These internal stresses could also be correlated with changes in the electrical polarization-voltage curves for the materials. It was shown that the combined effects of toughness and internal stress must be considered in choosing a material for an actual component.

ACKNOWLEDGMENTS

The support of the Office of Naval Research and Sandia National Laboratories during the course of this work is gratefully acknowledged. We would also like to thank R.C. Pohanka and R.H. Dungan who contributed many helpful ideas to these studies. The help of T.L. Baker and D. Heukeroth in collecting the data is also greatly appreciated.

REFERENCES

1. B. Jaffe, W.R. Cook, Jr., and H. Jaffe, "Piezoelectric Ceramics," Academic Press, New York (1971).
2. R.C. Pohanka, S.W. Freiman, and B.A. Bender, J. Am. Ceram. Soc. 61:72 (1978).
3. R.C. Pohanka, S.W. Freiman, K. Okazaki, and S. Tashiro in 5:353 "Fracture Mechanics of Ceramics," R.C. Bradt, A.G. Evans, D.P.H. Hasselman, and F.F. Lange, ed., Plenum, New York (1982).
4. R.F. Cook, S.W. Freiman, B.R. Lawn, and R.C. Pohanka, Ferroelectrics 50:267 (1983).
5. S.W. Freiman, D.R. Mulville, and P.W. Mast, J. Mater. Sci. 8:1527 (1973).
6. P. Chantikul, G.R. Anstis, B.R. Lawn, and D.B. Marshall, J. Am. Ceram. Soc. 64:539 (1981).
7. H. Igarashi and K. Okazaki, Japan-U.S. Seminar on Dielectric and Piezoelectric Ceramics (1982).
8. R.W. Rice and S.W. Freiman, J. Am. Ceram. Soc. 64:350 (1981).
9. R.W. Rice and R.C. Pohanka, J. Am. Ceram. Soc. 62:559 (1979).
10. I.J. Fritz and J.D. Keck, J. Phys. Chem. Solids 39:1163 (1978).
11. R.K. Spears, Ferroelectrics 37:653 (1981).
12. K. Kuroda and A. H. Heuer, Proc. of 41st Annual Meeting of Micros. Soc. of America, San Francisco Press, San Francisco, CA (1983).
13. R.H. Dungan and L.J. Storz, submitted to J. Am. Ceram. Soc.

FRACTURE BEHAVIOR OF CERAMICS USED IN MULTILAYER CAPACITORS

THERESA L. BAKER AND STEPHEN W. FREIMAN
National Bureau of Standards, Gaithersburg, MD 20899

ABSTRACT

This study involved the determination of the effects of composition and microstructure on the fracture toughness and susceptibility to environmentally enhanced crack growth of several ceramic materials used in multilayer capacitors. Indentation-fracture procedures were used to measure K_{IC} as well as to assess the possible effects of internal stresses on the fracture behavior of these materials and to correlate dielectric aging phenomena with strength. The environmentally enhanced crack growth behavior of these materials was determined by conducting dynamic fatigue tests in water.

INTRODUCTION

Mechanical failure of ceramic capacitors can be a serious problem from the point of view of loss of components during fabrication as well as the possibility of in-service failures. Freiman and Gonzalez [1] showed that flaw growth in a multilayer ceramic capacitor could lead to electrical breakdown due to the formation of a shorting path between two electrode layers. This type of behavior is thought to be the cause of the so-called "low voltage" failures [2]. The initial cracks can be the result of thermal stresses from soldering, machining damage, or improper handling.

The purpose of this study was to determine the effect of both chemical composition and microstructure on the resistance to crack growth under inert conditions (K_{IC}) as well as in environments known to enhance crack growth rates, such as water. A second objective was to determine whether internal stresses due to the paraelectric to ferroelectric phase transformation have an effect on the fracture of capacitor ceramics to the extent that they do in polycrystalline barium titanate [3,4]. Additionally, we hoped to determine whether there is a correlation between the rate at which the dielectric constant in certain capacitors decreased with time (dielectric aging) and the magnitude of internal stresses.

EXPERIMENTAL PROCEDURE

Materials

Six capacitor ceramics materials[1] designated Z5U, X7R-1, X7R-2, NPO, a Z5U material having a high dielectric aging rate and a Z5U material having a low dielectric rate were used in this study. The materials were processed identically to actual capacitors except that no electrode layers were introduced, in order to avoid the complications of crack/electrode interactions [1]. They were recieved as as-fired 25x25 mm squares. The thicknesses of the squares ranged from 1.0 to 1.8 mm from group to group with thickness variations of .02 to .29 mm within a group. The specimens were not completely flat but the test procedures were such that the small amount of warpage should not have affected the results. The general composition and grain sizes of the materials are given in Table 1.

---

[1] Supplied by the AVX corporation.

Table I

Compositions and Properties of Capacitor Ceramics

Designation	Composition[1]	Grain Size (μm)	K_{IC} ($MPam^{1/2}$)	n
NPO	Rare Earth Oxides	1-3	1.4	99 ± 48
X7R-1	$BaTiO_3$ (Bi)	≤1	1.1	85 ± 60
X7R-2	$BaTiO_3$	≤1	0.7	158 ± 212
Z5U	$BaTiO_3$	3-7	0.7	58 ± 10
Z5U "high" aging	$BaTiO_3$	3-7	1.1	
Z5U "low" aging	$BaTiO_3$	3-7	0.9	

[1] Major constitutent

Fracture Measurements

A Vickers indenter in a standard hardness tester was used at room temperature to introduce a controlled flaw at the center of each square. Indentation loads ranging from .3 to 100 N were used for the inert strength tests, while a 5 N indentation load was used for all the dynamic fatigue tests.

In the case of inert strength measurements, a drop of "dry" silicone oil was placed on the indentation site. (Dry refers to oil that was baked at 100°C for about 48 hours and was then placed in a dessicator until use.) The specimen was then immediately broken in biaxial tension with the tension side containing the indent. The test fixture consisted of a punch and three ball configuration with inner and outer spans of 4 and 20 mm respectively [5]. This test fixture was placed in a universal test machine and loaded at a crosshead speed of 500 mm/min in order to minimize environmental effects. In order to obtain data at this loading rate, a piezoelectric amplifier, attached to the load cell, was employed. As the sample was loaded and broken, a trace was recorded and measured from an oscilloscope which was connected to the piezoelectric cell.

Samples for the dynamic fatigue tests were also broken in biaxial tension using the same test fixture as before but in this case the tension side of the sample was submerged in water. Failure times ranged from several milliseconds for the fastest crosshead speed of 50 mm/min to a few hours for the slowest speed of .0005 mm/min. Six crosshead speeds, varying by an order of magnitude with respect to each other, were used. A piezoelectric cell was used for the two fastest tests while a standard load cell and chart recorder were used for the slower speeds.

A scanning electron microscope was used to examine the fracture pattern and morphology of the fracture surface of each of the six ceramic materials.

BACKGROUND

The indentation fracture procedure has been modeled by Chantikul et. al [6]. They showed that the critical stress intensity factor, K_{IC}, can be determined from the indentation load, P, and the fracture stress, σ, measured under inert conditions, through the following expression:

$$K_{IC} = \eta_v^R \left(\frac{E}{H}\right)^{1/8} \left(\sigma P^{1/3}\right)^{3/4} \quad (1)$$

where E is the elastic modulus of the material, H is the hardness, and η_v^R is an empirical constant determined experimentally to be 0.59 for a range of materials [6]. For this study, we took E to be 100 GPa (the elastic modulus of barium titanate) and H to be 8 GPa. However, the weak dependence of K_{IC} on E and H means that even moderate variations from these values would have little effect on the final results. Note that based on Equation 1, a logarithmic plot of σ versus P should yield a straight line of slope -1/3.

The susceptibility of ceramic materials to moisture enhanced crack growth is usually determined by a dynamic fatigue procedure in which the strength of the material in water is measured as a function of stressing rate. The underlying assumption to this procedure is that flaws in the material will grow slowly under the simultaneous presence of a stress and a reactive environment such as water. When the flaw grows to a size such that the stress intensity at the crack tip is equal to K_{IC}, failure will occur. Fuller et al. [7] showed that in dynamic fatigue, failure from a Vickers indentation induced flaw could be characterized by the following expression:

$$\sigma_f = (\lambda' \dot{\sigma}_A)^{\frac{1}{(n'+1)}} \quad (2)$$

where λ' is a constant which varies with the indentation load, and n' depends on the material and test environment. Fuller et al. showed that the value of n' associated with environmentally enhanced fracture from the indentation flaw is related to the value of n in the absence of a residual contact stress.

$$n = \frac{4}{3} n' - \frac{2}{3} \quad (3)$$

where n is the exponent in the expression for crack velocity, V:

$$V = V_o \left[\frac{K_I}{K_{IC}}\right]^n \quad (4)$$

and V_o is an empirical constant.

RESULTS AND DISCUSSION

Results will be presented in three sections. First we will examine the direct effects of composition and microstructure on strength and fracture toughness. Fracture behavior will be discussed in terms of the possible effects of internal stresses as an additional driving force for failure. Secondly, the possible relationship between dielectric aging and internal stresses will be presented. Finally, we will discuss the susceptibilty of these various ceramics to water enhanced crack growth.

Microstructure and Composition

As noted in the Background section of this paper, logarithmic plots of inert strength versus indentation load should yield straight lines of slope -1/3. Such plots are shown in Figure 1 for the Z5U, NPO, and the two X7R materials. Each data point represents an average of 5 specimens. Each specimen was examined optically after failure to ensure that fracture had indeed originated from the indentation site. Some materials, e.g. Z5U, exhibited more scatter than others. Nevertheless, over the range of indentation loads from 1N to 100N, all of these materials appear to follow the indentation model.

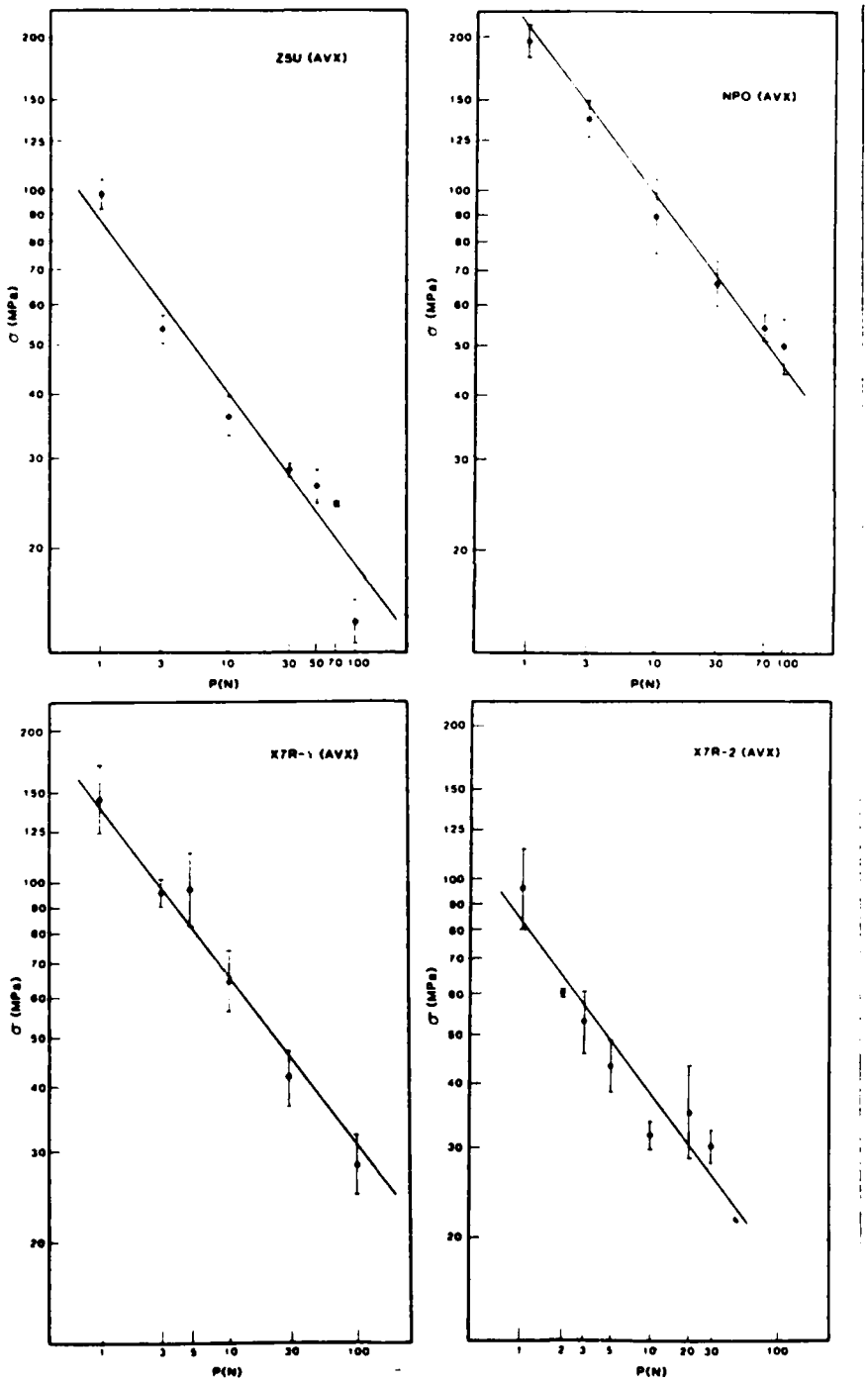

Figure 1. Inert strength data for Z5U, NPO, X7R-1, and X7R-2 capacitors. The curves are the best fit lines to the data plotted as a function of Vickers indentation load. Slope = - 1/3, according to Equation 1.

Contrast the above behavior with that observed in both a commercial and an experimental polycrystalline barium titanate developed for piezoelectric applications [3]. In this case, while the material in the paraelectric (cubic) state follows the indentation model over the entire range of loads, in the ferroelectric (tetragonal) state, there are clear deviations to lower strengths from this model at small indentation loads. This deviation is ascribed to the direct effect on the controlled flaw of internal stresses induced by the cubic to tetragonal phase transformation. The tensile components of these stresses exert an additional driving force on flaws whose size is comparable to that of the grains in the material. That the effect of such stresses is considerably smaller in capacitor materials is not surprising since these materials are at most, weakly piezoelectric. However, we will see later that these stresses cannot be completely discounted in terms of their effects on both fracture and dielectric aging.

As indicated by Equation 1, the positions of the curves in Figure 1 are a measure of the resistance of the material to crack growth, i.e. K_{IC}. The values of K_{IC} calculated from Equation 1 are given in Table 1. We can see that there are significant differences between the various materials. As an example, the presence of bismuth (Bi) in the X7R-1 compared to the X7R-2 material led to an increase in K_{IC}. Whether this is a direct effect of the change in composition or is related to the effect of the bismuth on the microstructure is not clear at present.

An examination of the fracture surface of these materials gives us a clue as to some of the reasons for these differences. As seen in Figure 2, the fracture surfaces of the four materials exhibit a varying degree of roughness implying that there are differences in the amount of crack deflection from one material to another. These data are in qualitative agreement with a model developed by Faber and Evans [8,9], which predicts increases in fracture toughness as the angle of crack deflection increases.

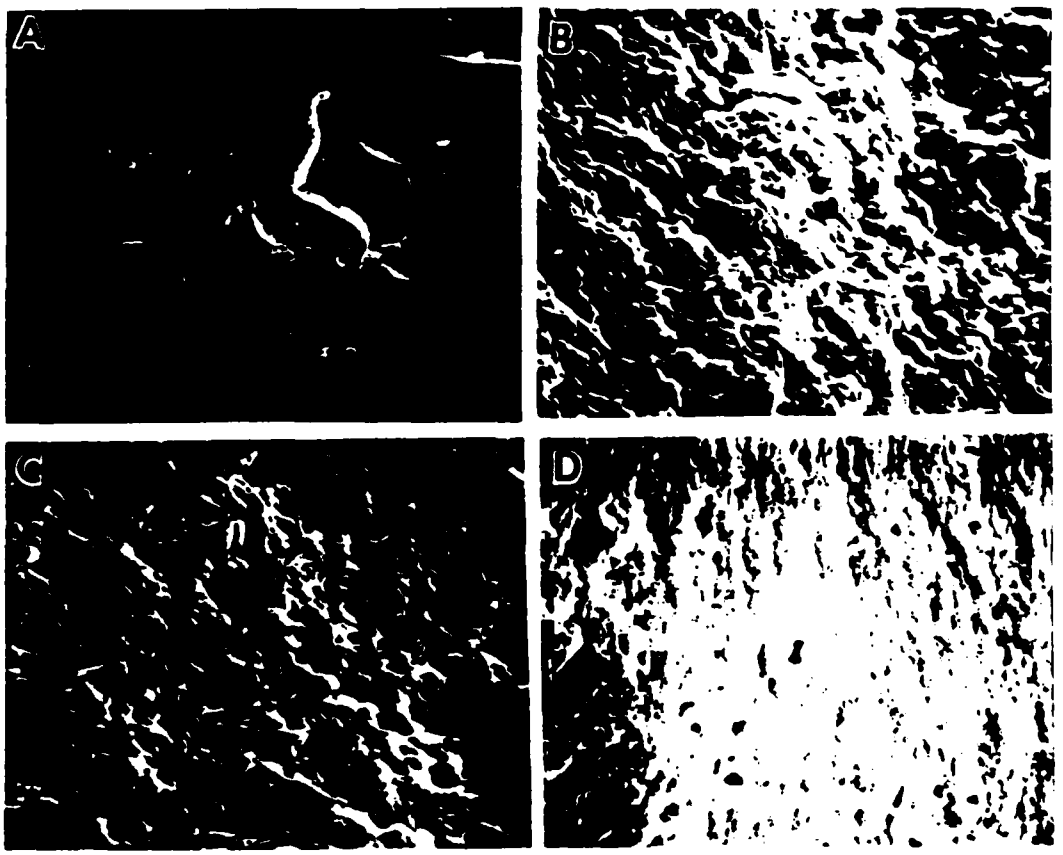

Figure 2. Scanning electron micrographs of the fracture surfaces for (A) Z5U, (B) NPO, (C) X7R-1, and (D) X7R-2

Correlation Between Strength And Aging

The dielectric constant of ferroelectric materials such as barium titanate is known to decrease with time, a process known as aging. There have been numerous theories put forth to explain this process. One model for dielectric aging in polycrystalline barium titanate which is in agreement with experimental observations, is that the decrease in the dielectric constant with time is due to the relief of internal stresses by the nucleation of 90° domains on already existing 90° domain boundaries [10]. The greater the magnitude of the internal stresses, the greater is the driving force for aging and the higher is the dielectric aging rate.

The results of indentation-strength experiments conducted on two Z5U capacitor materials having a "high" and "low" aging rate (Figure 3) tend to support the above hypothesis that internal stress levels can be related to rates of aging. By carrying out the indentation-strength measurements at smaller indentation loads (0.3 N) than those shown in Figure 1, it is possible to see differences in behavior between the two different materials. The position of the best fit $P^{-1/3}$ line for the two materials indicates that the "high" aging rate composition has the greater macroscopic toughness (1.1 compared to 0.9 $MPam^{1/2}$). (The 30 N point for the "low" aging rate material is thought to be high due to lateral cracking.) More importantly, the deviation of the 0.3 N data points from the indentation model appears to be a function of material. Earlier it was noted that this type of deviation in ferroelectric barium titanate has been ascribed to the presence of internal stresses in the material. If we take the difference between the fracture strength predicted by the indentation model at P = 0.3 N and that actually measured at this point as being proportional to the magnitude of the effective internal stress, we find that the effective internal stresses in the "high" aging rate material are approximately 2.5 times that for the "low" aging rate ceramic (90 MPa compared to 39 MPa). According to Bradt and Ansell [10], this internal stress difference would qualitatively explain the difference in aging rates.

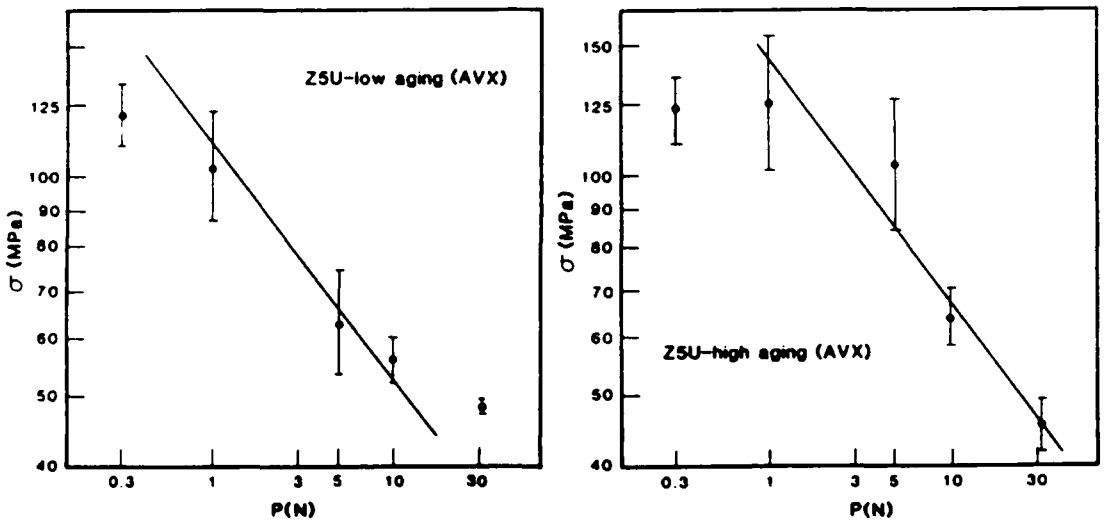

Fig. 3. Inert strength data for the "high" and "low" aging rate Z5U materials as function of indentation load.

A further experiment was conducted to elucidate the relationship between dielectric aging and mechanical stresses in these types of materials. A number of specimens of both the "high" and "low" aging rate ceramics were heated to 150°C and cooled to room temperature. These specimens were then indented using a 0.3 N load, and fractured under inert conditions at various times up to six days following the heat treatment. In order to obtain

strengths at the shortest times it was necessary to indent some specimens before heat treatment. Cook et al. [3] showed that strengths were not altered by heating indented barium titanate specimens above the Curie temperature and cooling to room temperature.

The strengths of the "high" and "low" aging rate specimens are plotted as a function of aging time in Figure 4. The absolute values of strength are slightly less than those shown in Figure 3, perhaps because the surfaces were modified somewhat by the thermal treatment. Within the scatter, these data show no apparent time dependence to the failure stress in either material, indicating that internal stresses are not being relieved. These data suggest that the driving force for aging does not decrease significantly with time, in agreement with the predictions of Bradt and Ansell [10].

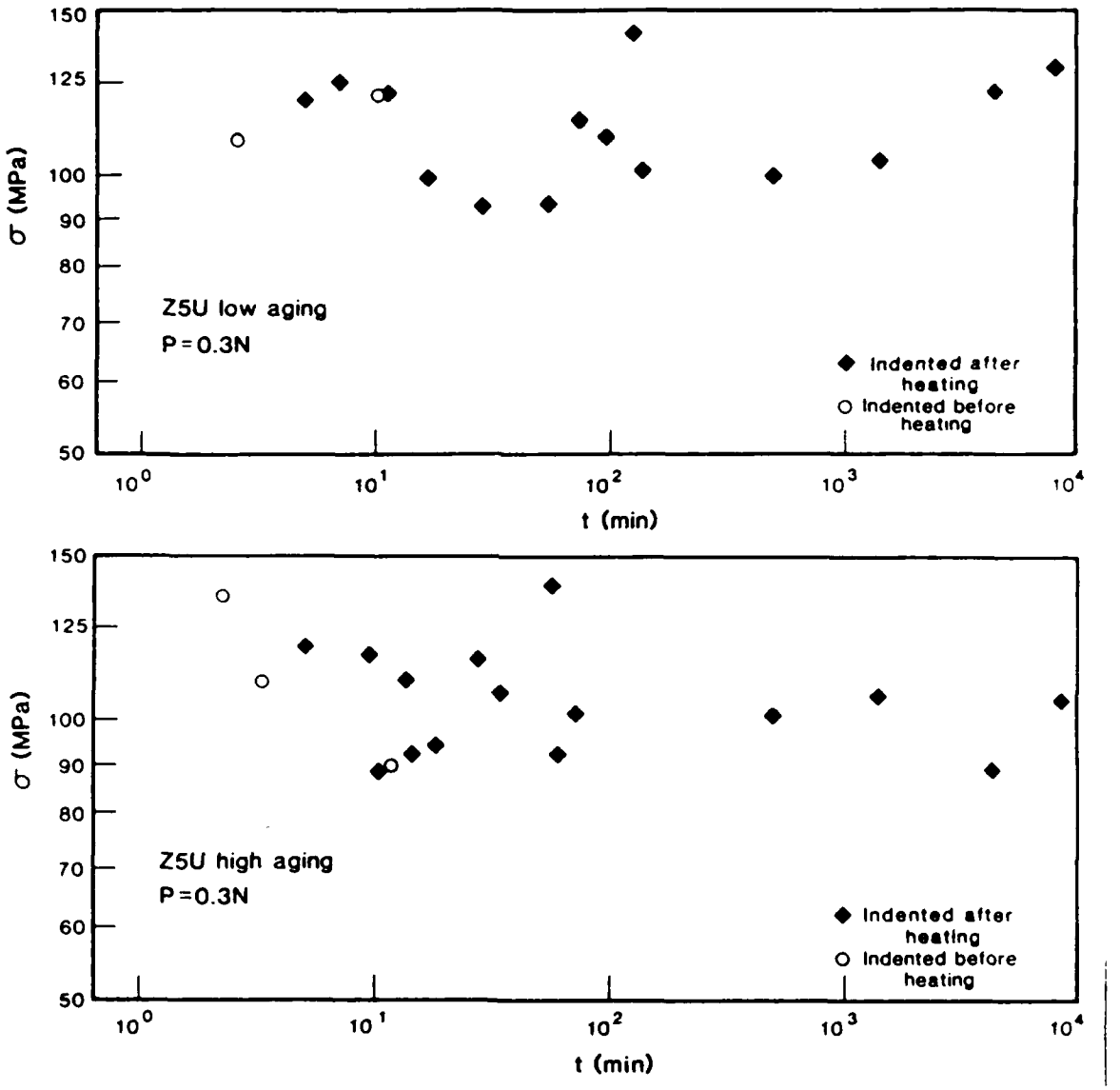

Figure 4. Inert strength data for the "high and "low" aging rate Z5U materials as a function of aging time. Indentation load was 0.3 N.

Environmental Effects

The dynamic fatigue data for the four capacitor compositions (Z5U, NPO, X7R-1, and X7R-2) are given in Figure 5. The data were fitted with a straight line based upon Equation 2. Each data point in Figure 5 is an average of 5

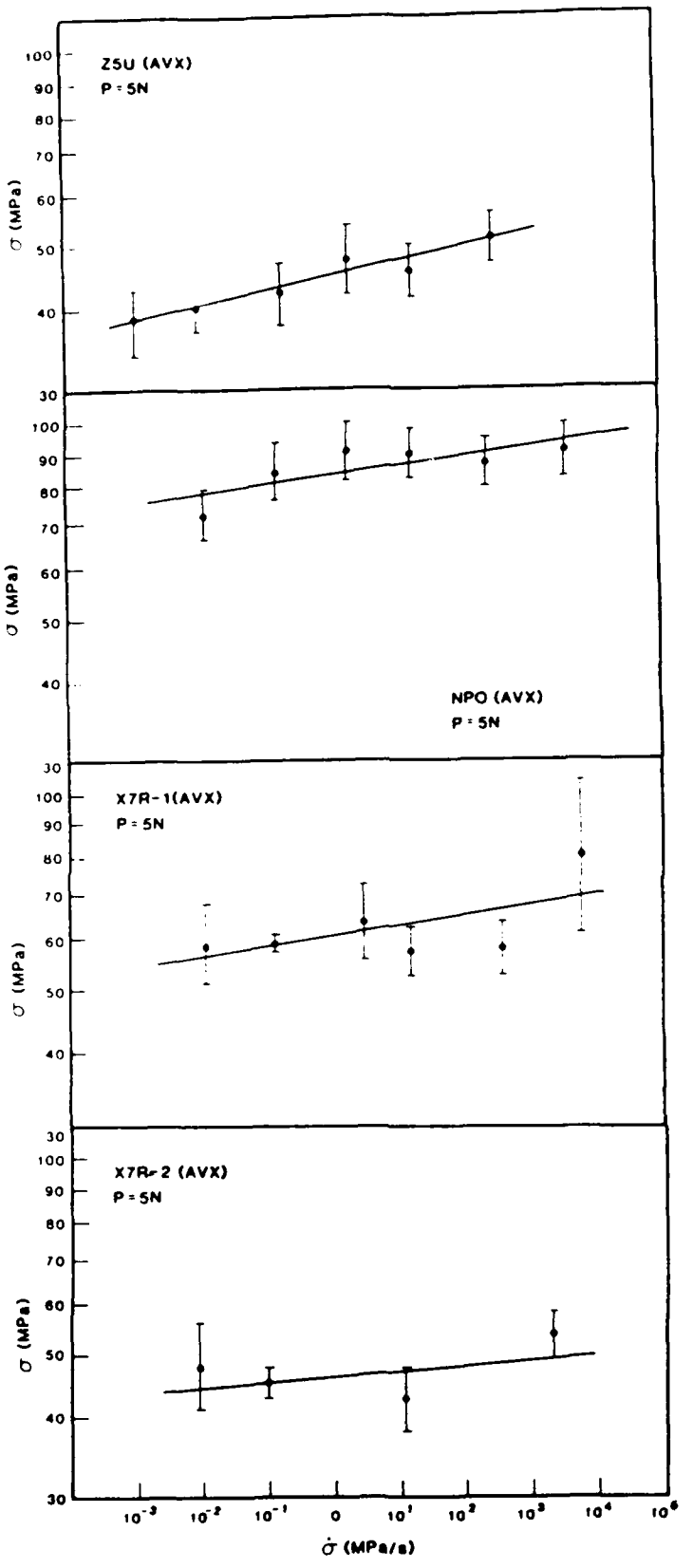

Figure 5. Dynamic fatigue data for Z5U, NPO, X7R-1, and X7R-2 in water as a function of stressing rate. Indentation load was 5 N. Lines were fit to the means at each stressing rate.

tests. The error bars are the standard deviation of the mean for that loading rate. The crack growth exponents, n, calcuated from this line using Equations 2 and 3 are given in Table 1. Based on the numbers alone, one can see that there is a significant difference in environmentally enhanced crack growth susceptibility among the four materials. Examining the plots more carefully reveals that there may be more fundamental differences in behavior.

First, notice that except for the Z5U material, there is a fair amount of scatter in the fit of the experimental data to the line. This scatter is reflected in the large standard error in the n values in Table 1. The increasing uncertainty in n as the value of n increases is normally observed. What is particularly unusual is the behavior of the two X7R materials. In both of these sets of data, if the highest stressing rate point is ignored, one would calculate an infinite value of n, an obviously impossible condition based upon the underlying assumptions of Equation 2. One hypothesis which would explain this dynamic fatigue data is the existence of a crack growth limit at a fairly high value of stress intensity compared to K_{IC}. The presence of a crack growth limit would give rise to a crack velocity - K_I curve like that shown schematically in Figure 6. At K_I's less than the value marked $K_{I(Limit)}$ in this diagram, no crack growth will occur. From an engineering point of view this would mean that at stresses below a given value, no mechanical failures or electrical breakdown due to cracks growing to form a short between two electrodes would occur. However, experimental proof of the existence of such a limit in these materials is needed. Clearly, more work is also needed in determining the relationship between the composition of the capacitor material and its susceptibility to crack growth.

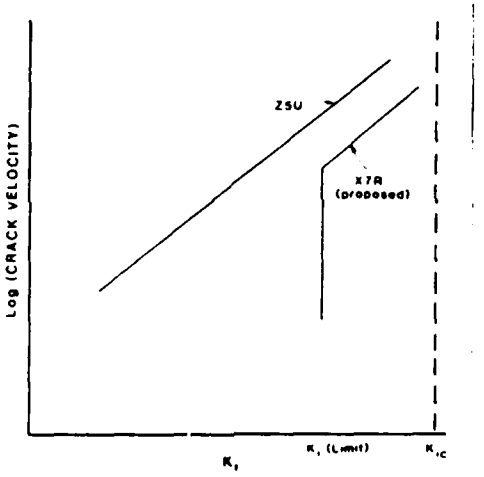

Figure 6. Schematic of hypothesized V-K_I curves for Z5U and X7R ceramics which would give rise to the dynamic fatigue behavior seen in Figure 5.

SUMMARY

Indentation-fracture techniques were used to determine the effects of composition and microstructure on the strength and environmentally enhanced crack growth in a number of capacitor ceramics. It was shown that the critical fracture toughness is quite variable from one material to another. The differences in K_{IC} are ascribed to variations in the degree of crack deflection. Little or no direct effects of internal stresses were observed in these materials except at indentation loads of 0.3 N or less, where it was shown that a Z5U material designated as having a "high" aging rate exhibited a stronger effect of internal stresses than did a "low" aging rate material. No measurable changes in these internal stress effects could be detected as a function of aging time.

Susceptibility to moisture enhanced crack growth was also shown to be a strong function of capacitor composition. The data for two X7R compositions suggested the existence of a crack growth limit in these materials.

ACKNOWLEDGEMENTS

We would like to thank the Office of Naval Research for their support of this work. We would also like to thank AVX Corp. and especially Lisa Kelley for supplying the specimens without which this work could not have been done. The helpful discussions with Bob Pohanka, Manfred Kahn, and Ed Fuller are also gratefully appreciated.

REFERENCES

1. S.W. Freiman and A.C. Gonzalez, to be published in Proc. Am. Ceramic Soc.

2. K. Sato, Y. Agato, K. Ohno, and H. Ikeo, Proc. of 18th Int. Reliability Physics Program, 212 (1980)

3. R.F. Cook, S.W. Freiman, B.R. Lawn, and R.C. Pohanka, Ferroelectrics 50, 267 (1983)

4. R.C. Pohanka, S.W. Freiman, and B.A. Bender, J. Am. Ceram. Soc 61, 72 (1978)

5. J.B. Wachtman Jr., W. Capps, and J. Mandel, J. of Mat. 7, 188 (1971)

6. P. Chantikul, G.R. Anstis, B.R. Lawn, and D.B. Marshall, J. Am. Ceram. Soc., 64, 539 (1981)

7. E.R. Fuller, Jr., B.R. Lawn, and R.,F. Cook, J. Am. Ceram. Soc., 66, 314, (1983)

8. K.T. Faber and A.G. Evans, Acta Met., 31, 565 (1983)

9. ibid, 577

10. R.C. Bradt and G.S. Ansell, J. Am. Ceram. Soc., 52, 192 (1969)

SECURITY CLASSIFICATION OF THIS PAGE (When Data Entered)

REPORT DOCUMENTATION PAGE		READ INSTRUCTIONS BEFORE COMPLETING FORM
1. REPORT NUMBER	2. GOVT ACCESSION NO.	3. RECIPIENT'S CATALOG NUMBER
4. TITLE (and Subtitle) Stress Corrosion of Ceramic Materials		5. TYPE OF REPORT & PERIOD COVERED Annual 1 Oct 1984 - 31 Sept 1985 6. PERFORMING ORG. REPORT NUMBER
7. AUTHOR(s) S. W. Freiman, G. S. White, T. L. Baker, S. M. Wiederhorn, T. D. Coyle and L. Chuck		8. CONTRACT OR GRANT NUMBER(s) N00014-85-F-0021
9. PERFORMING ORGANIZATION NAME AND ADDRESS National Bureau of Standards Ceramics Division, Room A331, Bldg. 223 Gaithersburg, MD 20899		10. PROGRAM ELEMENT, PROJECT, TASK AREA & WORK UNIT NUMBERS
11. CONTROLLING OFFICE NAME AND ADDRESS Office of Naval Research 800 N. Quincy Street Arlington, VA 22217		12. REPORT DATE 1 Aug 1986 13. NUMBER OF PAGES
14. MONITORING AGENCY NAME & ADDRESS(if different from Controlling Office)		15. SECURITY CLASS. (of this report) 15a. DECLASSIFICATION/DOWNGRADING SCHEDULE
16. DISTRIBUTION STATEMENT (of this Report)		
17. DISTRIBUTION STATEMENT (of the abstract entered in Block 20, if different from Report)		
18. SUPPLEMENTARY NOTES		
19. KEY WORDS (Continue on reverse side if necessary and identify by block number) Crack growth; fracture; stress corrosion; ceramics; glasses; capacitors		
20. ABSTRACT (Continue on reverse side if necessary and identify by block number) The critical fracture energy and susceptibility to environmentally enhanced fracture were shown to depend on the bonding in single crystals. Fracture energy results agreed with predictions based on force laws. Additions of lithium to basic solutions reduced crack growth rates in silica by over an order of magnitude. K_{Ic} and subcritical crack growth in capacitor ceramics were a function of composition and microstructure. Correlations between strength and dielectric aging rate were obtained for a Z5U capacitor material.		

DD FORM 1 JAN 73 1473 EDITION OF 1 NOV 65 IS OBSOLETE
S/N 0102-LF-014-6601

SECURITY CLASSIFICATION OF THIS PAGE (When Data Entered)

END

12-86

DTIC